Solid Earth

Evolution of structures and hydrothermal alteration in a Palaeoproterozoic supracrustal belt: Constraining paired deformation–fluid flow events in an Fe and Cu–Au prospective terrain in northern Sweden

Joel B. H. Andersson[1], **Tobias E. Bauer**[1], **and Edward P. Lynch**[2]

[1]Division of Geosciences and Environmental Engineering, Luleå University of Technology, 971 87 Luleå, Sweden
[2]Department of Mineral Resources, Geological Survey of Sweden, P.O. Box 670, 751 28 Uppsala, Sweden

Correspondence: Joel B. H. Andersson (joel.bh.andersson@ltu.se)

Abstract. An approximately 90 km long Palaeoproterozoic supracrustal belt in the northwestern Norrbotten ore province (northernmost Sweden) was investigated to characterize its structural components, assess hydrothermal alteration–structural geology correlations, and constrain a paired deformation–fluid flow evolution for the belt. New geological mapping of five key areas (Eustiljåkk, Ekströmsberg, Tjårrojåkka, Kaitum West, and Fjällåsen–Allavaara) indicates two major compressional events (D_1 and D_2) have affected the belt, with each associated with hydrothermal alteration types typical for iron oxide–apatite and iron oxide Cu–Au systems in the region. Early D_1 generated a regionally distributed, penetrative S_1 foliation and oblique reverse shear zones that show a southwest-block-up sense of shear that formed in response to NE–SW crustal shortening. Peak regional metamorphism at epidote–amphibolite facies broadly overlaps with this D_1 event. Based on overprinting relationships, D_1 is associated with regional scapolite ± albite, magnetite + amphibole, and late calcite alteration of mafic rock types. These hydrothermal mineral associations linked to D_1 structures may form part of a regionally pervasive evolving fluid flow event but are separated in this study by crosscutting relationships.

During D_2 deformation, folding of S_0–S_1 structures generated F_2 folds with steeply plunging fold axes in low-strain areas. NNW-trending D_1 shear zones experienced reverse dip-slip reactivation and strike-slip-dominated movements along steep, E–W-trending D_2 shear zones, producing brittle-plastic structures.

Hydrothermal alteration linked to D_2 structures is a predominantly potassic–ferroan association comprising K-feldspar ± epidote ± quartz ± biotite ± magnetite ± sericite ± sulfides. Locally, syn- or post-tectonic calcite is the main alteration mineral in D_2 shear zones that intersect mafic rocks. Our results highlight the importance of combining structural geology with the study of hydrothermal alterations at regional to belt scales to understand the temporal–spatial relationship between mineralized systems. Based on the mapping results and microstructural investigations as well as a review of earlier tectonic models presented for adjacent areas, we suggest a new structural model for this part of the northern Fennoscandian Shield. The new model emphasizes the importance of reactivation of early structures, and the model harmonizes with tectonic models presented by earlier workers based mainly on petrology of the northern Norrbotten area.

1 Introduction

The northern Norrbotten area of Sweden is an economically important metallogenic province and mining district (Weihed et al., 2008). For example, about 90 % of European iron ore is annually produced in the area from two of the world's largest underground iron mines at Kiirunavaara and Malmberget (LKAB, 2017; OECD, 2017). These world-class deposits (combined current reserves of ca. 1051 Mt at 43.4 % Fe; LKAB, 2017) comprise iron oxide–apatite (IOA)

or "Kiruna-type" mineralization, with the Kiirunavaara deposit representing the archetypal example (e.g. Geijer, 1910, 1930). The Aitik Cu–Ag–Au deposit also occurs in northern Norrbotten and is one of the largest open-pit copper mines in Europe (current resource of ca. 801 Mt at 0.22 % Cu, 1.3 g t^{-1} Ag and 0.15 g t^{-1} Au; New Boliden AB, 2017). Aitik represents an enigmatic porphyry-style deposit with a protracted ore-forming history that is thought to include an overprinting iron oxide–copper–gold (IOCG)-style mineralization event (e.g. Wanhainen et al., 2005, 2012). Beyond the active mines, numerous Fe and Cu ± Au prospects and deposits occur, making the area one of the most prospective terrains in Europe for IOA- and IOCG-style deposits (e.g. Carlon, 2000; Billström et al., 2010; Martinsson et al., 2016).

Palaeoproterozoic supracrustal belts in Norrbotten are significant from a metallogenic perspective as they preferentially host a variety of base and precious metal ores and thus represent key exploration targets (e.g. Carlon, 2000; Martinsson, 2004). In detail, syn-orogenic "Svecofennian" sequences deposited between ca. 1.90 and 1.87 Ga represent a key stratigraphic horizon that locally hosts significant IOA- and IOCG-style deposits (Romer et al., 1994; Edfelt et al., 2005; Smith et al., 2007; Wanhainen et al., 2012; Westhues et al., 2016). Both deposit types commonly occur within or immediately adjacent to large-scale deformation zones, which traverse and follow the supracrustal belts, suggesting these zones and their contained lithologies strongly influenced strain localization.

Palaeoproterozoic supracrustal rocks in northern Norrbotten also preserve evidence of regional- and local-scale hydrothermal alteration and fluid–rock interaction (e.g. Romer, 1996; Frietsch et al., 1997; Edfelt et al., 2005; Bernal et al., 2017), and share broad lithological, structural, and alteration characteristics with other IOCG and IOA prospective terrains worldwide. For example, features such as variably distributed sodic and potassic alteration, the bimodal character of host volcanic rocks, the spatial proximity of deformation zones, and Cu–Au mineralization conform with the IOCG mineral system model defined by Skirrow et al. (2019) and mimic the character of other IOCG-mineralized terrains in Brazil (e.g. deMelo et al., 2017; Craveiro et al., 2019), Australia (e.g. Skirrow et al., 2019), Canada (e.g. Corriveau and Mumin, 2010; Corriveau et al., 2016),and Mauritania (e.g. Kolb et al., 2008). Therefore, further studies of IOA and IOCG prospective terrains in northern Sweden may contribute to an improved understanding of the formation of these deposit types, provide new insights into the broader controls on mineralization, and help refine conceptual ore-forming or exploration models applicable to geographically isolated and underexplored supracrustal domains in northern Fennoscandia, or analogous terrains elsewhere.

The deposition of Orosirian supracrustal rocks, collectively referred to as "Svecofennian" (e.g. Gaal and Gorbatschev, 1987), marks the onset of the Palaeoproterozoic Svecokarelian orogeny (ca. 1.96–1.75 Ga) in Sweden. Previous studies of Svecofennian supracrustal rocks in northern Norrbotten have included provincial compilations to ascertain lithostratigraphic and petrogenetic insights (e.g. Frietsch, 1984; Pharaoh and Pearce, 1984; Forsell, 1987; Perdahl and Frietsch, 1993; Bergman et al., 2001) and local studies constraining the geological, geochemical, geophysical, and/or structural character of sequences hosting Fe and Cu ± Au deposits (e.g. Geijer, 1910, 1920, 1930, 1950; Parák, 1975; Edfelt et al., 2006; Sandrin and Elming, 2006; Smith et al., 2007; Wanhainen et al., 2012; Westhues et al., 2016, 2017; Bauer et al., 2018). With a few exceptions (Wright, 1988; Bergman et al., 2001; Grigull et al., 2018; Luth et al., 2018; Lynch et al., 2018a, b), regional compilations have tended to lack structural information. Local studies with a structural component (e.g. Edfelt et al., 2006; Debras, 2010; Wanhainen et al., 2012) generally have not considered the broader significance of deposit-proximal structures in reconstructing deformation and/or fluid flow events for individual belts or the wider region. Thus, deformation-zone- or belt-scale investigations that include a coupled structural–alteration assessment may provide new insights into the number and character of paired deformation–hydrothermal events affecting a given supracrustal belt.

In this paper, we present new structural and alteration mapping of a deformed and metamorphosed Orosirian supracrustal belt located about 40 km to the west of Kiruna in northwest Norrbotten, northern Sweden (Figs. 1, 2, and 3). The studied sequence, herein referred to as the Western Supracrustal Belt (WSB; cf. Wright, 1988), extends for about 90 km in a NNW–SSE direction and hosts several Fe and Cu ± Au occurrences (e.g. Offerberg, 1967; Witschard, 1975; Edfelt et al., 2005; Frietsch, 1974). New geological mapping of five key domains is used to ascertain the type, geometry, kinematics, and interrelationships of various structural components within the belt and thus constrain its structural evolution. Additionally, a petrographic and paragenetic study of mappable hydrothermal alteration zones associated with different lithotypes and/or structures is used to constrain the character and number of fluid flow events within the supracrustal rocks and attempts to link these hydrothermal events to specific phases of deformation. Overall, this coupled structural–alteration approach provides a new unifying deformation model for the Western Supracrustal Belt, identifies key structural controls on hydrothermal alteration (and by inference Fe and Cu ± Au mineralization), and establishes an updated space–time framework for Svecokarelian deformation and hydrothermal fluid flow in this sector of northern Fennoscandia.

For simplicity, the prefix "meta" for various metamorphic rocks (e.g. metarhyolite) is not used in this paper as all rocks have been metamorphosed to some degree (Bergman et al., 2001). We also follow the recommendations of the Committee for Swedish Stratigraphic Nomenclature for geological and stratigraphic naming conventions (Kumpulainen, 2007).
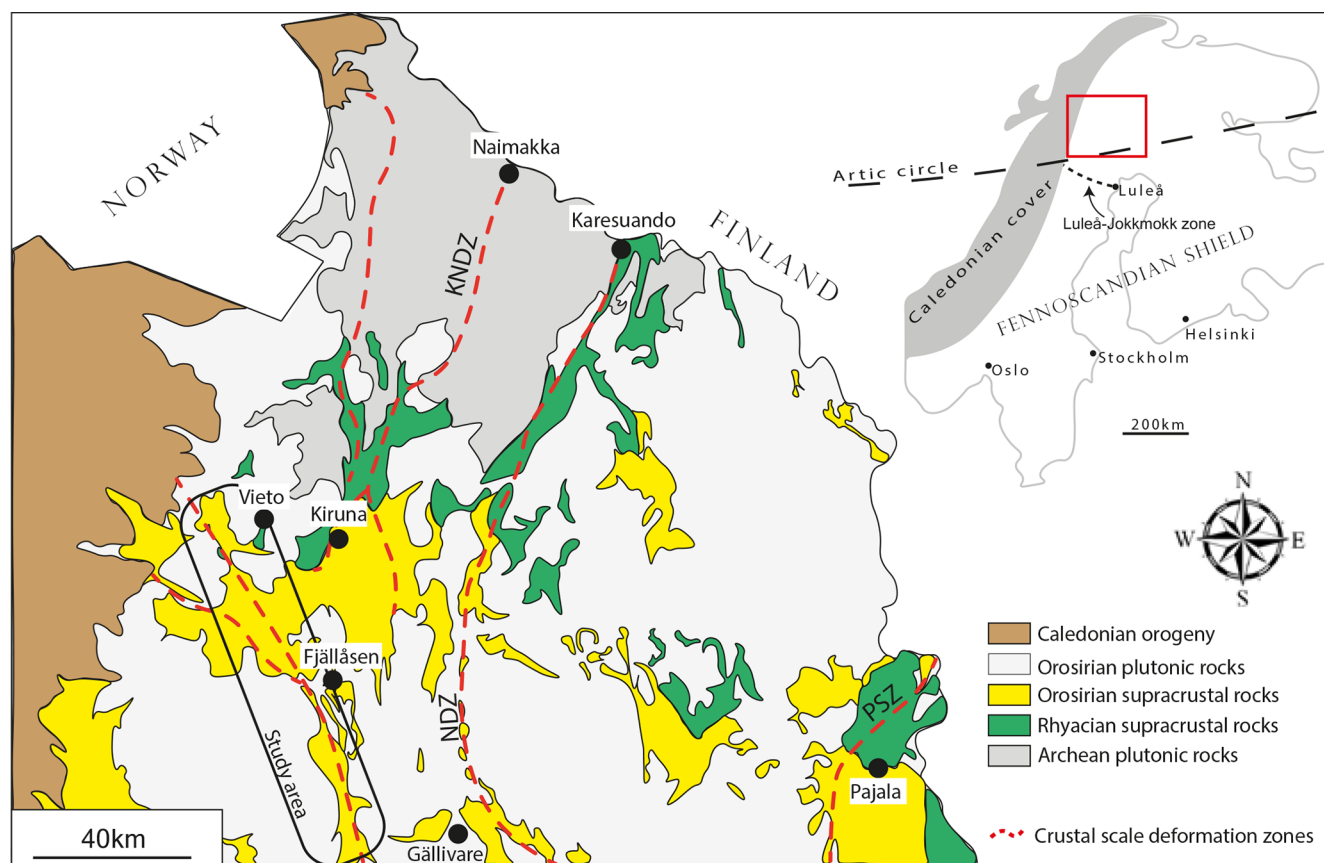
Figure 1. Generalized geology of northern Norrbotten highlighting Palaeoproterozoic supracrustal belts. Simplified and modified after Bergman et al. (2001).

2 Regional geological setting

The northern Fennoscandian Shield (Fig. 1) is underlain by a continental nucleus of Archean (ca. 2.9–2.6 Ga) granitic, tonalitic, and amphibolitic gneisses (Gaal and Gorbatschev, 1987; Lahtinen et al., 2008). Rifting of this continental basement between ca. 2.5 and 2.1 Ga developed crustal-scale, rift-parallel fault basins and voluminous tholeiitic mafic magmatism and related sedimentation, producing an approximately NW-aligned large igneous province extending from northern Norway to Russia (Pharaoh and Pearce, 1984; Hanski et al., 2012; Melezhik and Hanski, 2012; Bingen et al., 2015). In northern Sweden, Archean rocks belong to the Norrbotten Craton, one of three continental nuclei that were rifted during the Rhyacian and later reassembled during the Svecokarelian accretionary–collisional orogenic cycle in the Orosirian (e.g. Lahtinen et al., 2005, 2008). In northern Norrbotten (Fig. 1), Rhyacian rift basalt and related mafic igneous and sedimentary rocks constitute the lowermost part of the Palaeoproterozoic stratigraphy (Fig. 4) and occur within several NNE- and NNW-trending greenstone belts (e.g. Martinsson, 1997; Melezhik and Fallick, 2010; Lynch et al., 2018a).

Early Svecokarelian-cycle orogenic magmatism (ca. 1.90–1.86 Ga) in northern Sweden generated two regional suites of co-magmatic volcano-plutonic rocks that are divisible based on petrological, geochemical, and geographical considerations (Fig. 4). In the east, calc-alkaline intermediate to felsic volcanic–volcaniclastic rocks and co-magmatic dioritic to granodioritic intrusions predominate (i.e. porphyrite group and Haparanda intrusive suites in Fig. 4). In the west, mildly alkaline (shoshonitic), intermediate to felsic volcanic–volcaniclastic rocks and co-magmatic monzonitic intrusions occur (i.e. Kiirunavaara group and Perthite monzonite intrusive suites in Fig. 4). Late Svecokarelian-cycle magmatism in northern Norrbotten generated widespread I-to A-type granitic plutonism (Edefors suite in Fig. 4) and coeval S-type granites (Lina suite in Fig. 4) ca. 1.81–1.78 Ga in response to eastward subduction as part of the Transscandinavian Igneous Belt (Andersson, 1991; Åhäll and Larsson, 2000; Weihed et al., 2002; Högdahl et al., 2004; Rutanen and Andersson, 2009).

In general, metamorphic facies and related pressure–temperature (P–T) estimates are poorly constrained throughout northern Norrbotten (e.g. Bergman et al., 2001; Skelton et al., 2018), but at least two regional metamorphic

events (Fig. 4) that broadly correspond to the early- and late-orogenic cycles are reported (Bergman et al., 2001, 2006; Bergman, 2018; Sarlus et al., 2017). Based on metamorphic mineral associations and microprobe data, Bergman et al. (2001) suggested that the regional metamorphic grade increases from greenschist to amphibolite facies conditions from west to east. East of the Western Supracrustal Belt (Fjällåsen; Figs. 1, 2, 3), syn-orogenic volcanic rocks yielded P–T values of 4.0–7.5 kbar and 630–805° (i.e. amphibolite to granulite facies; Bergman et al., 2001). The uppermost granulite facies P–T estimate (7.5 kbar, 805 °C) was determined for a sedimentary rock within a high-strain deformation zone and bounded by ca. 1.8 Ga granites, and may represent contact metamorphic conditions around the granite plutons and/or the effects of retrograde reactions (Bergman et al., 2001).

In the Gällivare area (Fig. 1), shear-zone-hosted schists along the Nautanen deformation zone (NDZ) have yielded P–T values of 2.5–4.3 kbar and 589–681 °C (i.e. amphibolite facies; Tollefsen, 2014). Also in the Gällivare area, Romer (1996) reported a U–Pb age of 1730 ± 6.4 Ma for fracture-hosted stilbite in volcanic rocks, suggesting this area has remained below the closure temperature of stilbite (ca. 150 °C) since ca. 1.73 Ga. A possible regional resetting of the Rb–Sr isotopic systems at ca. 1.6–1.5 Ga (e.g. Welin et al., 1971; Skiöld, 1979) is recorded by ca. 1.9–1.8 Ga magmatic rocks in northern Norrbotten (Fig. 4). In central Sweden, ca. 1.6–1.5 Ga rapakivi intrusions occur (Andersson, 1991; Andersson, et al., 2002), but magmatic and/or hydrothermal ages in Norrbotten are not known during this time span; hence, the geological significance of the isotope resetting remains unclear.

Palaeoproterozoic rocks in northern Norrbotten record evidence of a complex, polyphase deformation history that evolved predominantly in response to Svecokarelian orogenesis (D_1 and D_2 in Fig. 4) and involves at least two regional deformation events (e.g. Vollmer et al., 1984; Forsell, 1987; Wright, 1988; Bergman et al., 2001; Bauer et al., 2018; Grigull et al., 2018; Luth et al., 2018; Andersson, 2019). In the Kiruna area, Wright (1988) argued for an early D_1 thrusting event overprinted by gentle local folding and shear zone development (D_1 to D_4 in Wright 1988). For the same area, Andersson (2019) ascribed the earliest Svecokarelian compressional deformation to basin inversion and proposed four major deformation phases to explain the structural configuration in the Kiruna area (D_1–D_4 in Fig. 4). Bergman et al. (2001) argued for two regional deformation events (D_1 and D_2) in northern Norrbotten, and Bauer et al. (2018) described a pronounced gneissic S_1 cleavage affected by F_2 folding in the Gällivare area (Fig. 1), implying two deformation events.

The maximum age of the earliest D_1 event in Kiruna is constrained at 1880 ± 3 Ma by Cliff et al. (1990) based on a zircon U–Pb TIMS (thermal ionization mass spectrometry) age for an undeformed granophyre dyke cutting the Ki-

irunavaara IOA deposit. A similar timing for D_1 has been inferred based on deformation intensity recorded by ca. 1.89–1.88 Ga as well as 1.88–1.86 Ga plutonic rocks in northern Norrbotten (Bergman et al., 2001). The timing of the regional D_2 tectonic event is generally constrained by the emplacement of syn- to late-orogenic, ca. 1.8 Ga granites and related hydrothermal activity (e.g. Bergman et al., 2001; Smith et al., 2009; Bauer et al., 2018). The D_4 event in Fig. 4 corresponds to maximum ages of ca. 1740 and 1620 Ma for open fractures in the Gällivare area (Romer, 1996) and is the last documented Proterozoic deformation in that area (Bauer et al., 2018).

3 Geology of the Western Supracrustal Belt

3.1 Setting, extent, and lithotypes

The Western Supracrustal Belt refers to a discontinuous, ca. 6 km wide by 90 km long, NNW-trending Orosirian (ca. 1.89–1.87 Ga) domain located to the west of Kiruna in northwestern Norrbotten (Figs. 2, 3). In an earlier study, Wright (1988) defined the WSB as a north–south-trending supracrustal inlier zone immediately to the west of Kiruna (i.e. the Eustiljåkk key area; Figs. 2, 3). However, this area represents the northernmost part of a larger supracrustal terrain that extends further southward to the west and southwest of the Kiruna and Gällivare mining areas. In this study, we retain the original nomenclature of Wright (1988) but expand the term "Western Supracrustal Belt" to include the areas from Allavaara-Fjällåsen in the south to Eustiljåkk in the north that are underlain by Orosirian supracrustal rocks (Figs. 2, 3). Similar lithostratigraphic domains occur to the west of the WSB as relatively small inliers surrounded by Palaeoproterozoic plutonic rocks or as tectonic windows surrounded by Palaeozoic rocks (e.g. Angvik, 2014).

In general, the geology of the WSB is dominated by calc-alkaline to alkaline, volcanic–volcaniclastic rocks with basaltic to rhyolitic compositions that were metamorphosed at approximately peak epidote–amphibolite facies conditions (Ros, 1979; Bergman et al., 2001; Edfelt et al., 2006). Along its margins, the WSB is bound by subordinate ca. 1.88–1.86 Ga granodioritic to dioritic plutonic rocks and more abundant ca. 1.80 Ga granites (Bergman et al., 2001). The plutons intrude, truncate, and disrupt the supracrustal pile; this aspect, combined with the polydeformed nature of the sequence, makes lateral stratigraphic correlations difficult. In the Ekströmsberg area (Figs. 2, 3), Rhyacian greenstones are found at the margin of the belt, providing a partly persevered pre- to syn-orogenic stratigraphic record (Offerberg, 1967; Witschard, 1975). In the Allavaara area (Figs. 2, 3), Witchard (1975) indicated synclinal folds comprised Rhyacian greenstones on their flanks and Orosirian felsic to intermediate volcanic rocks in their cores.
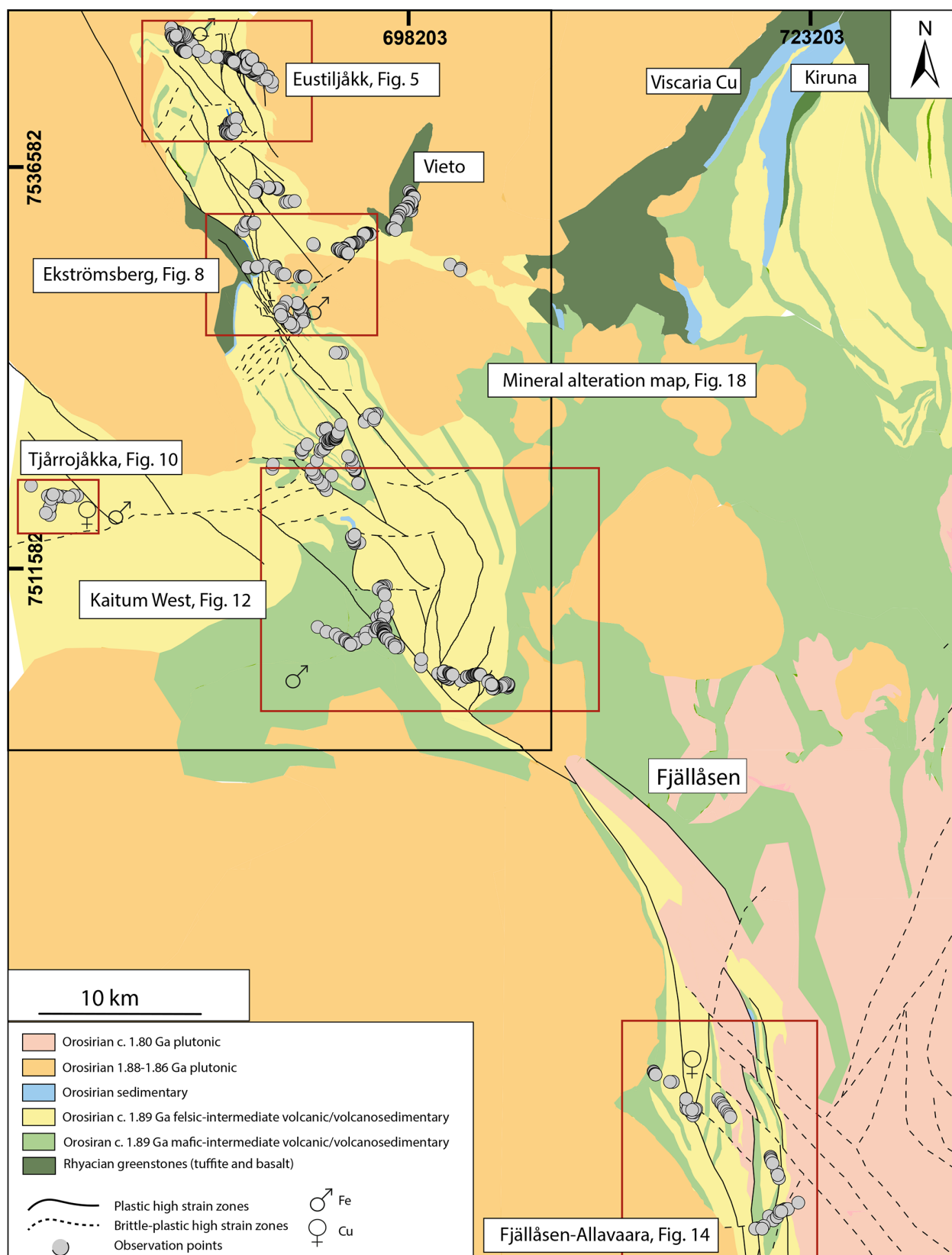
Figure 2. Geological map of the Western Supracrustal Belt showing the key areas mapped during this study. Lithological contacts simplified and modified after Offerberg (1967), Witschard (1975), and Bergman et al. (2001). Coordinates: Sweref99.
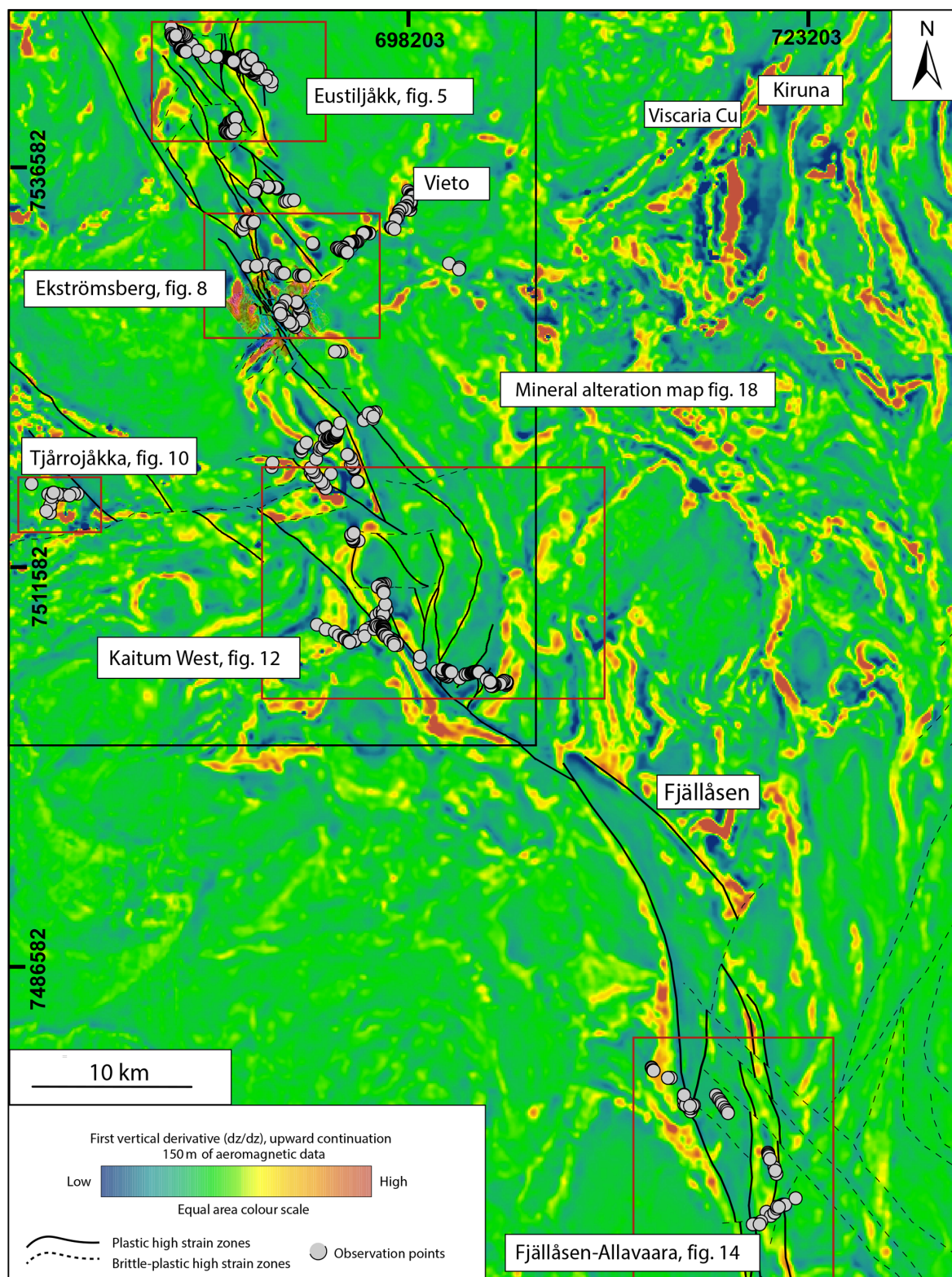
Figure 3. First vertical derivative, 150 m upward continuation, aeromagnetic map of the Western Supracrustal Belt overlain by first vertical derivative ground magnetic map of Ekströmsberg. The aeromagnetic data were collected using 200 m line spacing and 40 m down-line distance (Bergman et al., 2001). The ground magnetic data were collected using ≤ 80 m line spacing and ≤ 20 m down-line distance (Frietsch et al., 1974). Outline of the key areas, observation points, and dominant structures are the same as in Fig. 2. Data from Frietsch et al. (1974) and Bergman et al. (2001). Coordinates: Sweref99.
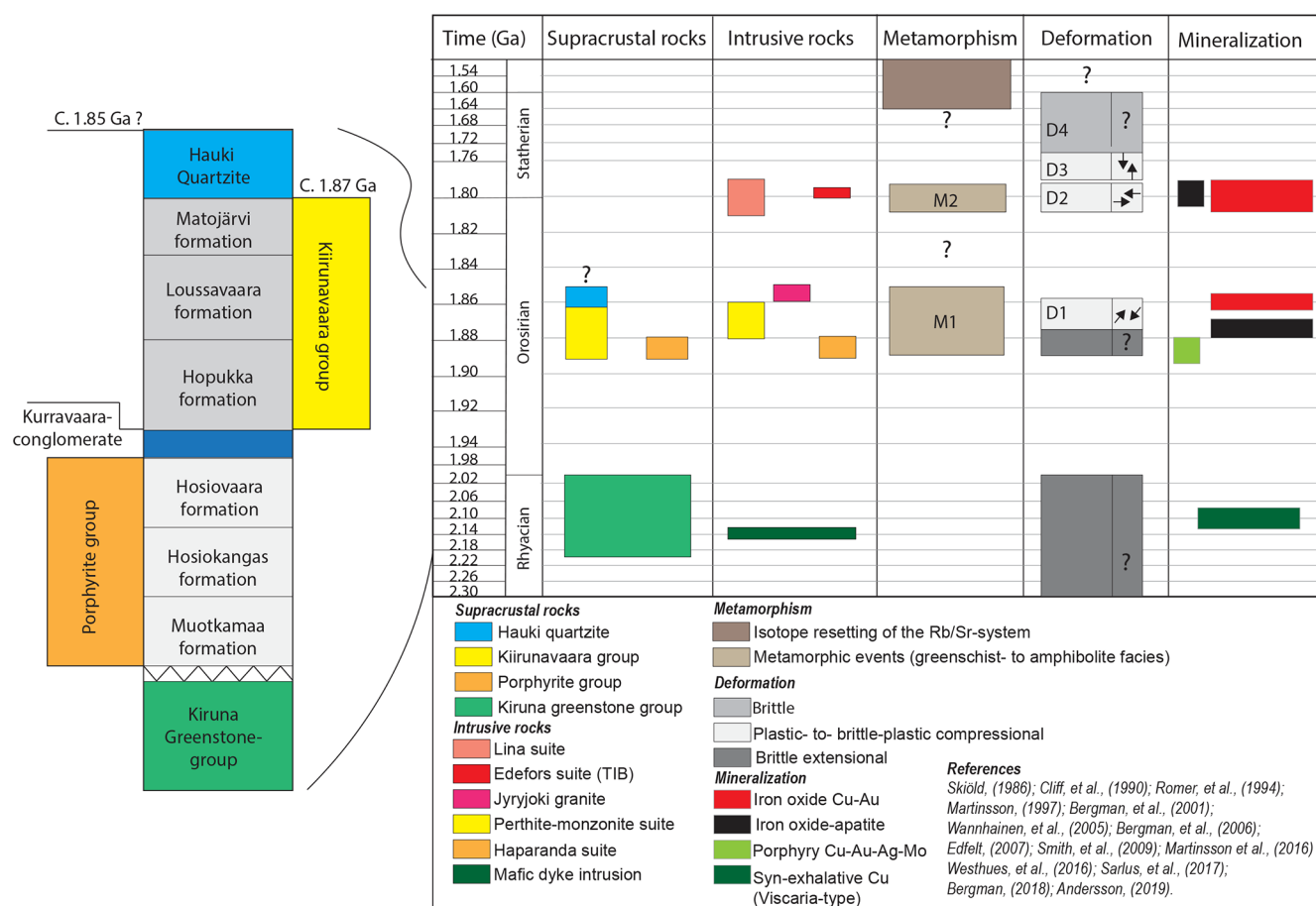
Figure 4. Summary of the temporal relation between supracrustal/intrusive rocks, metamorphism, deformation, and mineralization in northern Norrbotten. Stratigraphic column of the supracrustal sequence relevant for this study is included.

3.2 Structural geology

Previous studies incorporating parts of the WSB provide a partial and somewhat contradictory assessment of its structural character and evolution (cf. Wright, 1988; Bergman et al., 2001; Edfelt et al., 2006). At Eustiljåkk in the northern WSB (named *Ruojtatjåkka South* in Wright, 1988), Wright (1988) identified a steep, NW-trending mylonite zone that mimics the NNW orientations of high-strain zones at Allavaara to the south (Figs. 2, 3). The Eustiljåkk mylonite provides kinematic evidence for a west-side-down, oblique normal sense of shear, based on rotated porphyroclasts with asymmetric tails (Wright, 1988). In contrast, Bergman et al. (2001) report overall west-side-up kinematics for the composite shear zone within the WSB based on outcrop observations west of Kiruna and Gällivare (Fig. 1). A set of ENE-trending dextral strike-slip shear zones in the Eustiljåkk area (*Ruojtatjåkka South* in Wright, 1988) have also been reported by Wright (1988), who suggested these structures post-date the dominant NNW–SSE tectonic grain.

Based on airborne (Bergman et al., 2001) and ground magnetic data (Frietsch et al., 1974), several prominent NNW-trending linear magnetic anomalies occur along the WSB, or as splay anomalies extending NW to WNW towards the Tjårrojåkka area (Fig. 3). These lineaments are assigned to an unnamed, crustal-scale Palaeoproterozoic shear zone, analogous to the major NE-trending Karesuando–Arjeplog deformation zone to the northeast and the NNW-trending Nautanen deformation zone to the east (e.g. Bergman et al., 2001; Sandrin and Elming, 2006). Moreover, the magnetically anomalous character of the WSB mimics similar "striped" magnetic signatures associated with intense magnetite alteration and mylonitic deformation within the better-understood IOCG-mineralized Nautanen deformation zone to the east (Fig. 1; e.g. Lynch et al., 2015, 2018b), giving relevance to regional comparisons.

3.3 Mineralization and related alteration

Both iron oxide–apatite (IOA) and hydrothermal Cu ± Au mineralization occurs along the WSB. The best-documented examples are the Tjårrojåkka Fe–Cu system (e.g. Edfelt et al., 2005, 2006) in the west and the Ekströmsberg IOA deposit (Frietsch, 1974) in the east (Figs. 2, 3). The

Tjårrojåkka system (Edfelt et al., 2005, 2006) comprises a western IOA deposit and an IOCG-style Cu ± Au ore-body in the east. The IOA deposit is primarily associated with pervasive albite + scapolite + magnetite ± amphibole alteration, while "red rock"-style potassic–ferroan (K-feldspar + hematite ± albite) alteration is mainly associated with the Cu deposit (Edfelt et al., 2005). The Ekströmsberg deposit comprises several parallel NW-trending magnetite and hematite orebodies. The orebodies are associated with sericite + quartz-altered host volcanic rocks and discordant calcite veining, as well as muscovite, zircon, epidote, tour-maline, and allanite as probable secondary accessory matrix minerals (Frietsch, 1974).

In general, Fe and Cu mineralization along the WSB ap-pears to be partly controlled by superimposed structures formed during polyphase deformation. In the Tjårrojåkka area, Edfelt et al. (2006) report three main deformation events; D_1 and D_2 generated cleavages in NE- and E-oriented shear zones, respectively, and a later D_3 event folded D_1 structures and produced shallow SE-striking cleavages dipping towards the southwest. Additionally, the Fe and Cu orebodies at Tjårrojåkka are aligned with D_1 NE- to ENE-trending planar structures (Edfelt et al., 2006). At the Ek-strömsberg IOA deposit, Frietsch (1974) reported several prominent structures, including NW-trending schistosity par-allel to the orientation of the main orebodies. Additional structural components include locally developed folds, a ma-jor NW-trending and smaller NE-trending fault zones, and brecciated phenocrysts (Frietsch, 1974). Overall, these fea-tures imply a polyphase structural evolution for the Ek-strömsberg IOA deposit based on plastic fabrics intersected by brittle deformation zones. Further detailed descriptions of the structural characteristics of the Ekströmsberg IOA de-posit are presently lacking, however.

4   Methods

In this study, five key areas were chosen to study the structural differences and/or similarities along the WSB: Eustiljåkk, Ekströmsberg, Tjårrojåkka, Kaitum West, and Fjällåsen–Allavaara (Figs. 2, 3). Geological mapping with a structural focus was conducted between 2015 and 2017. A total of 698 outcrop observations were made, and 1079 structural measurements were collected. The mapping cam-paign covered all outcropping areas between Allavaara in the south and Eustiljåkk in the north (Figs. 1, 2), although it should be noted that the total outcrop exposure for the WSB is estimated at ca. 1–3 % by surface area. All structural mea-surements were collected using Brunton Geo Pocket Tran-sits, and the data were digitized in the field on ruggedized iPad mini devices using the application Field Move (formerly Midland Valley Exploration Ltd., currently Petroleum Ex-perts Ltd.). Lineations were measured as the pitch on planes and recalculated into true orientation using the software Geo

Calculator (Holcombe, Coughlin, Oliver, Valenta Global). For magnetite-rich rocks, structural measurements were es-timated using known distal points in the terrain. Structural analysis was performed using the Move 2017 software pack-age (formerly Midland Valley Exploration Ltd., currently Petroleum Experts Ltd.), whereas maps were constructed us-ing ArcMap (ESRI). Stereographic plots were produced as lower-hemisphere equal-area stereographic projections us-ing Dips 7.0 (Rocscience). Forty-one oriented samples were collected throughout the study area. The samples were cut across foliation and parallel to lineation and sent to Van-couver Petrographics Ltd. for thin-section preparation, one thin section per sample. Petrography and microstructural investigations were performed using a conventional petro-graphic polarization microscope equipped with a digital cam-era (Nikon ECLIPSE E600 POL).

Hydrothermal alteration mapping was conducted via field observations at the outcrop to hand sample scale using 10× hand lenses. We focused on the recognition of mappable al-teration mineral associations to establish possible links be-tween certain structures and alteration styles, and identify specific structural and/or alteration characteristics that may prove useful as a vectoring tool toward Fe and/or Cu min-eralization. The purpose of this approach was to provide a holistic overview of paired deformation–hydrothermal pro-cesses affecting the WSB, and this scientific contribution of-fers a starting point for further studies on the evolution of hydrothermal mineral alteration in this underexplored area.

5   Results

In general, the structural mapping results highlight two su-perimposed deformation events that generated plastic and brittle-plastic structures along the WSB that vary in terms of their character and intensity. Likewise, variably devel-oped hydrothermal alteration displays localized differences in terms of type, style, and intensity.

5.1   Eustiljåkk area

The Eustiljåkk area provides a relatively well-exposed ca. E–W profile across the northern WSB (Figs. 2, 5). The area pre-dominantly comprises weakly deformed porphyric volcanic rocks, along with subordinate sedimentary rocks and mafic dykes. Steep, west-dipping shear zone structures occur in the NE part of the area and impart a dominant N–S-trending structural grain (Fig. 5). Beyond this area to the west, other large-scale ca. NW-trending structures are interpreted from magnetic anomaly data (Bergman et al., 2001, Fig. 3). Al-though ground truthing of these western structures was not possible due to poor exposure, their continuity was verified by structural measurements and thin-section analysis of sim-ilarly deformed rocks along strike in key areas south of Eu-stiljåkk.
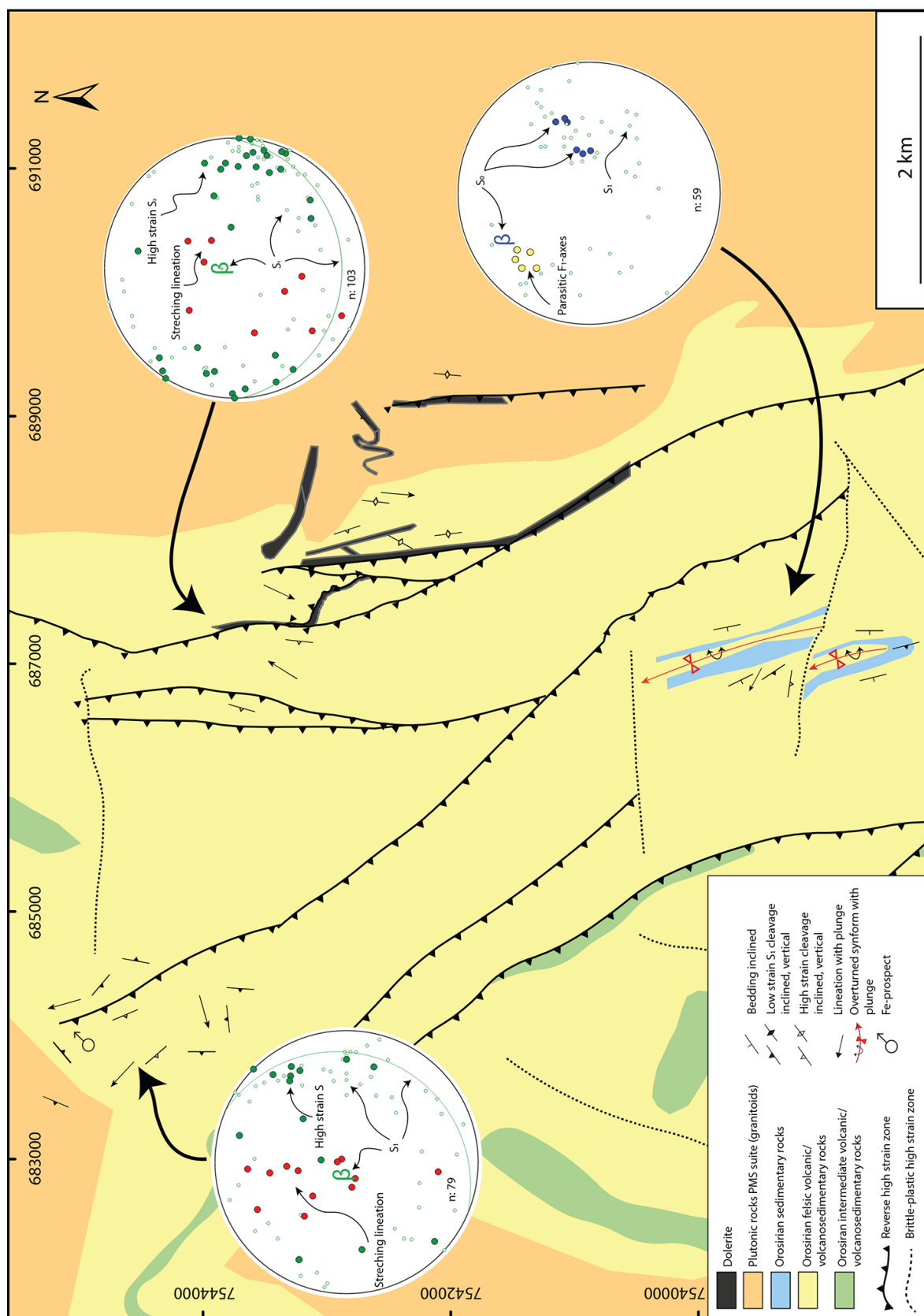
Figure 5. Geological map of the Eustiljåkk key area. Modified after Offerberg (1967). Coordinates: Sweref99.

In general, a weakly developed penetrative cleavage is present throughout the Eustiljåkk area. We designate this cleavage S_1 because it is folded into F_2 folds with near-vertically plunging fold axes (Fig. 5). NNW–SSE- or N–S-trending and west-dipping structural grains that are parallel with magnetic lineaments appear to control the orientation of S_1 cleavages (Figs. 5, 6). The magnetic map indicates that NNW–SSE-trending planar structures are the more dominant trend compared to N–S-oriented structures at Eustiljåkk (Figs. 3, 5), whereas stereographic projections of S_1 foliations indicate a N–S structural grain as dominant (Fig. 6). This contradiction likely reflects a greater surface exposure in outcropping areas containing ca. N–S-oriented planar structures, giving a greater number of structural measurements with N–S orientations as shown in the S_1 summary stereographic plot of the Eustiljåkk area (Fig. 6a–b).

S_1 foliation is defined by a preferred mineral orientation of feldspar + quartz ± biotite ± actinolite ± hornblende in intermediate to felsic volcanic rocks (Fig. 7a) and adjacent granitoids. The cleavage in the granitoids is unevenly distributed and is generally of low intensity. In the area between Eustiljåkk and Ekströmsberg (Fig. 2), calcite forms part of the foliated mineral association within porphyric volcanic rocks. In mafic rocks, S_1 is defined by actinolite + plagioclase ± epidote ± hornblende ± calcite that show a preferred mineral orientation parallel to the ca. N–S-aligned S_1 fabric.

In general, bedding surfaces (S_0) are only rarely preserved in the Eustiljåkk area. In the southern part (Fig. 5), deformed arkose horizons are interbedded with more competent volcanic porphyric rocks. The more western of these horizons is slightly steeper and shows intense NNE-verging parasitic F_1 folds with M and Z geometry (Fig. 7b). Based on bedding–bedding and bedding–cleavage relationships, combined with parasitic fold geometries, we interpret the larger-scale structure as a NE-verging, overturned synform. An axial planar S_1 cleavage locally associated with the F_1 folds strikes sub-parallel to bedding but is slightly steeper dipping (see inset stereoplots in Fig. 5). The calculated F_1 β axis (β: 330/15) plunges gently towards the northwest, which is comparable to the measured NW-plunging fold axes of parasitic F_1 Z folds (Fig. 5). F_1-fold limbs are transected by an E–W-trending high-strain zone in the southern Eustiljåkk area as inferred from the aeromagnetic map and supported by high-strain cleavage measurements near the magnetic lineament (Fig. 5). Axial planar S_1 appear to be locally transposed into this high-strain zone (Fig. 5). We interpret this phenomenon as localized transposition of S_1 and S_0 in response to D_2 shearing. In the northwestern part of the Eustiljåkk map sheet, a low-intensity S_1 cleavage is folded into inferred F_2 folds. Stereographic analysis indicates slightly asymmetrical fold geometries with a calculated β axis (β: 293/79) plunging steeply towards the northwest (Fig. 5). Corresponding F_2-fold hinges and axial planar cleavages (S_2) were not observed in the field or in thin sections.

The northeastern part of the Eustiljåkk area (Fig. 5) is characterized by mainly N–S- and subordinate NW–SE- and NE–SW-trending sets of thin, well-exposed high-strain zones. Stretching lineations show variable orientations (Fig. 5). In relatively low-strain units, S_1 cleavages plot near the best-fit plane (Fig. 5), suggesting F_2 folding around a calculated β axis plunging steeply to the north (β: 357/79), whereas high-strain fabrics (designated S_2) are oriented consistently N–S (Fig. 5). Mafic dykes are commonly encountered either within or at the contacts of the high-strain zones (Fig. 7c) and are interpreted to reflect magmatism during D_2 deformation. Locally, mafic dykes show internal folding of leucocratic material (possibly albititized dolerite), but relatively undeformed dykes also occur. The mafic dykes are in most cases not wider than a couple of metres and occur as swarms. The high-strain zones and related mafic dykes transect the granitoid pluton bordering the volcanic rocks in the east, implying granitoid emplacement occurred prior to D_2-related deformation and mafic magmatism.

Oriented thin sections did not yield any high-confidence kinematic indicators, making the kinematic interpretation of Eustiljåkk uncertain. Despite this, the east-verging F_1 fold in the southern part of the area (Fig. 5) suggests the Eustiljåkk area was affected by west-side-up movements during D_1.

5.2 Ekströmsberg area

The Ekströmsberg key area (Fig. 8) is dominated by felsic to intermediate volcanic rocks that host the Ekströmsberg IOA deposit (Frietsch, 1974). Dominant NNW–SSE-trending high-strain deformation zones west of the Ekströmsberg IOA deposit (Fig. 9) are poorly exposed and are mainly inferred from aeromagnetic and ground magnetic anomalies (Frietsch et al., 1974; Bergman et al., 2001). These magnetic anomalies can be linked to high-strain zones mapped just northwest of the Ekströmsberg IOA deposit (Fig. 9) and further south in the Kaitum West area (Fig. 12, Sect. 5.4).

A penetrative, continuous cleavage is defined by a preferred orientation of feldspar + quartz ± biotite ± amphibole (mean orientation: 251/50). We designate this fabric S_1 because its orientation is partly controlled by later D_2 structures (see below). S_1 fabrics are developed in both supracrustal and plutonic rocks, although ductile fabrics only sporadically occur in the latter. A mineral stretching lineation is generally present in felsic–intermediate volcaniclastic rocks and is defined by stretched feldspar and quartz. Occasionally, a well-developed mineral lineation (L_m) in mafic rocks is defined by actinolite–tremolite forming a distinct L tectonite (Fig. 9a). In general, however, LS tectonites are more commonly developed at Ekströmsberg.

Subordinate sedimentary rocks occur in the northwestern part of the Ekströmsberg area and mainly comprise poorly sorted, polymict conglomerate with poorly developed or indistinct bedding features (Fig. 8), at a stratigraphic position corresponding to the Kurravaara conglomerate (Fig. 4). Lo-
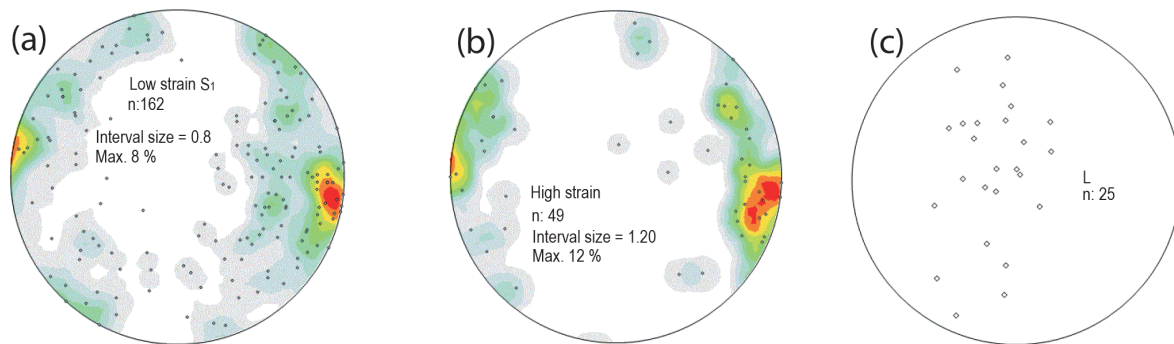
Figure 6. Stereographic equal-area projections highlighting **(a)** low-strain S_1, **(b)** high-strain S fabrics, and **(c)** stretching and mineral lineations.
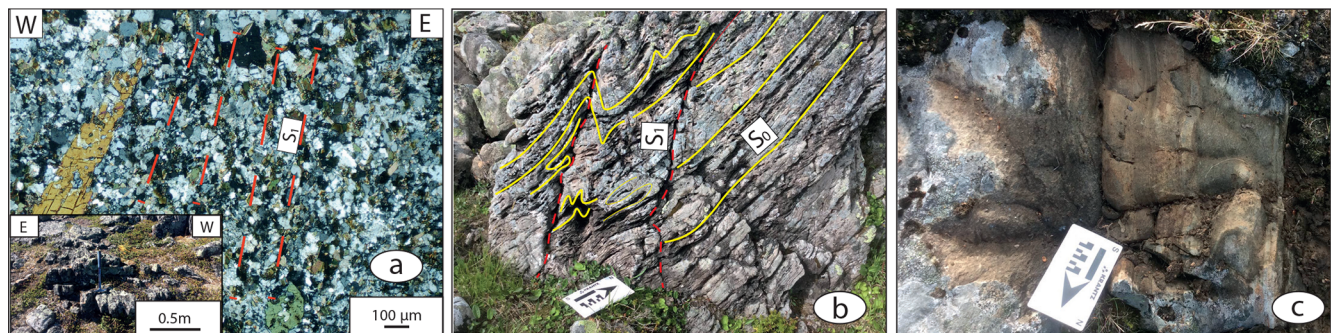

Figure 7. Characteristics of the Eustiljåkk key area. **(a)** Low-intensity S_1 foliation, X688743 Y7542711. **(b)** Parasitic F_1 folding of sedimentary horizons, X687043 Y7539378. **(c)** Scapolite-altered mafic dyke associated with N–S-directed high-strain zones, X687505 Y7543037. Coordinates: Sweref99.

cally, pillow basalt provides reliable bedding markers, especially where primary magmatic layering is indicated by stratiform scapolite replacement (Fig. 9b). Additionally, lithological contacts (Offerberg, 1967), structural lineaments derived from magnetic maps (Frietsch et al., 1974; Bergman et al., 2001), and measured fold axes (designated F_1) were used to infer fold geometries at Ekströmsberg (Fig. 8). In general, S_1 foliations are axial planar to F_1 folds with steep, south-plunging fold axes (Fig. 8). A low-intensity foliation of uncertain origin is commonly observed in felsic porphyric volcanic rocks (Fig. 9c, d). This planar fabric is defined by a preferred orientation of feldspar and quartz which locally resembles a tectonic cleavage, although pressure shadows and/or recrystallization around feldspar phenocrysts were not observed (Fig. 8d). We interpret this fabric as a primary (S_0) magmatic flow fabric which may correlate to what Frietsch (1974) described as "fluidal banded" volcanic rocks at Ekströmsberg (see Fig. 9 in Frietsch, 1974). In the southern Ekströmsberg area, the magmatic fabric evident in felsic volcanic rocks is folded into a tight, upright, and near-cylindrical F_1 fold with a steeply plunging fold axis (β: 195/75). A NNE-oriented, subvertical foliation is parallel to the fold's axial plane and is interpreted as an axial planar cleavage designated S_1.

Inferred S_1 cleavages in felsic volcanic–volcaniclastic rocks appear to be transposed into a set of subvertical, E–W-trending strike-slip- and NNW–SSE-trending reverse dip-slip shear zones near the Ekströmsberg IOA deposit (Fig. 8). We interpret this effect as the transposition of S_1 cleavage into later-formed shear zones (S_2), thus marking two compressional deformation events (i.e. D_1 and D_2). A mafic volcanic rock in the northwestern part of the key area shows a crenulation cleavage within a NNW–SSE-trending reverse dip-slip mylonite zone, which also suggests two fabric-forming events (Fig. 9e).

Shear sense determined from SCC' fabrics in thin sections of foliated volcanic rocks indicates oblique west- to southwest-side-up kinematics for the main NNW–SSE-trending high-strain zones at Ekströmsberg. Oblique sinistral (Fig. 9f) and reverse dip-slip (Fig. 9g) movements are recorded along moderately N- to NNW-plunging and subvertical stretching lineations respectively, with both suggesting overall west-block-up kinematics. Approximately E–W-trending mylonite zones in felsic volcanic rocks close to the Ekströmsberg IOA deposit (Fig. 8) show strike-slip movement with a sinistral top-to-the-west sense of shear as indicated by SC fabrics (Fig. 9h). No direct crosscutting relationships between the E–W- and NNW–SSE-trending high-strain
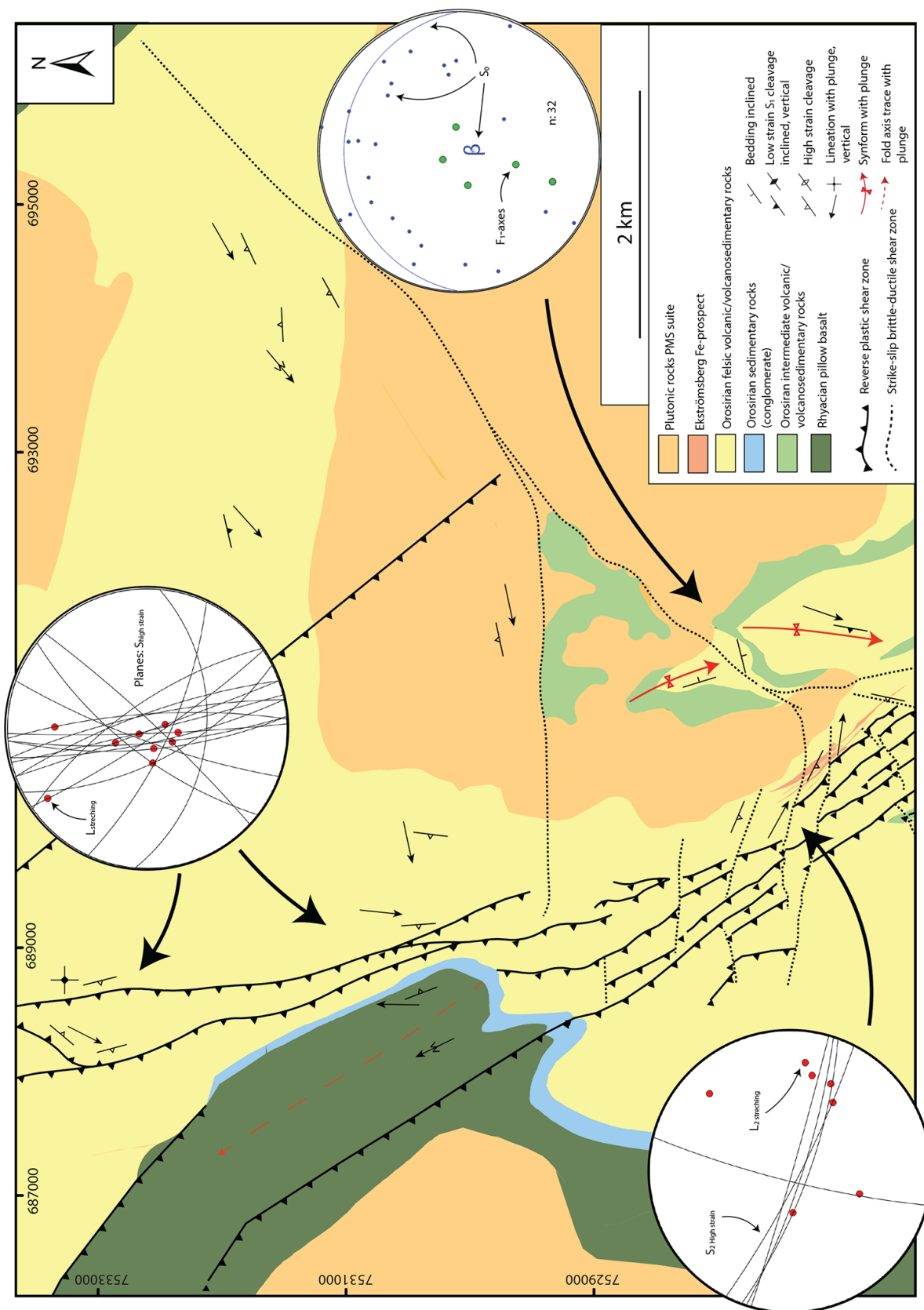
Figure 8. Geological map of the Ekströmsberg key area. Modified after Offerberg (1967). Coordinates: Sweref99.
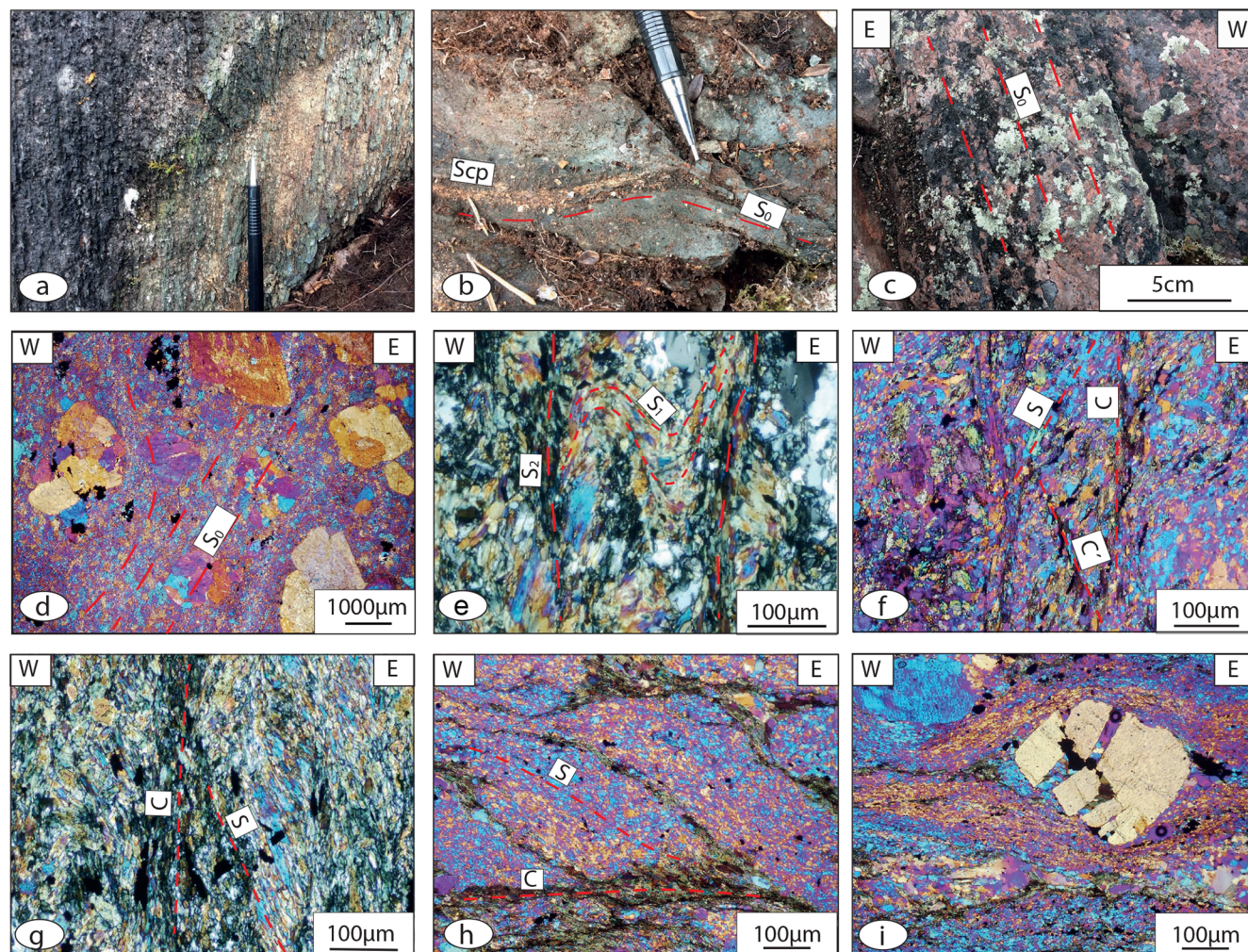
Figure 9. Field images and thin-section photographs of characteristics of the Ekströmsberg area. **(a)** Actinolite–tremolite L tectonite overprinted by calcite alteration, X689886 Y7530423. **(b)** Semi-conformable scapolite replacement of magmatic bedding in Rhyacian basalt, X688163 Y7530345. **(c)** Magmatic bedding in a felsic volcanic rock resembling a weak tectonic cleavage in outcrop, X691591 Y7527763. **(d)** Micrograph of the outcrop in **(c)**. **(e)** Micrograph of crenulation from same locality as **(b)**, X688163 Y7530345. **(f)** SCC′ fabric along north-plunging stretching lineation in the NNW-directed grain, X688714 Y7530350. **(g)** SC fabric along near-vertical stretching lineation in the NNW-directed grain, X688167 Y7530354. **(h)** SC fabric along shallow east-plunging stretching lineation along the E–W-directed grain, X690276 Y7527251. **(i)** Brittle feldspar along the E–W-directed grain, same location as **(h)**. Scp: scapolite. Coordinates: Sweref99.

zones were observed at the outcrop scale. However, E–W tectonic fabrics tend to offset NNW–SSE-oriented lineaments on magnetic maps along the WSB (Fig. 3), suggesting a later timing for E–W high-strain zones on a regional to belt scale.

Close to the Ekströmsberg IOA deposit, feldspar porphyroclasts found in felsic volcaniclastic rocks and transected by E–W high-strain deformation zones record the effects of brittle deformation (Fig. 9i). In contrast, this type of grain-scale brittle deformation was not observed in similar feldspar-phyric lithologies deformed by NNW–SSE-trending mylonite zones along the WSB. Rocks affected by both structural trends also show sub-grain rotation (SGR) quartz recrystallization textures with local bulging (BLG) recrystallization (cf. Fig. 9f, h, i). Overall, this textural evidence

suggests recrystallization proceeded at approximately 400 °C (Passchier and Trouw, 2005), although a slightly lower temperature (< 400 °C) is indicated by the brittle character of feldspar within the E–W-trending shear zones (Fig. 9i; cf. Passchier and Trouw, 2005).

5.3 Tjårrojåkka area

The Tjårrojåkka area (Fig. 10) mainly comprises felsic and intermediate volcaniclastic and volcanic rocks that host the Tjårrojåkka Fe–Cu system (cf. Edfelt et al., 2005). Primary bedding (S_0) is locally visible in laminated volcanosedimentary rocks and greywacke. Throughout the area, a visibly dominant penetrative planar foliation occurs and is gener-

ally oriented subparallel to S_0 bedding/laminae. This planar structure, here designated S_1, is defined by the alignment of amphibole, quartz, feldspar, and locally magnetite in the volcanic–volcaniclastic rocks and is axial planar to meso-scale intrafolial isoclinal folds (Fig. 11a). In the central part of the key area, S_0 bedforms are folded by a major ENE–WSW-aligned, isoclinal F_1-fold sequence which, based on its surface trace, shows apparent re-folding (Fig. 10). Mineral lineations are generally observable as an alignment of amphibole and quartz on S_1-foliation planes. Both bedding and S_1 foliations are overprinted by F_2 folds with axial traces trending approximately N–S to NE–SW (Fig. 10). F_2-fold geometries are upright, open to closed, and show a distinctive spaced cleavage that is parallel to their axial surface traces and is here designated S_2. The N- to NE-aligned S_2 cleavage is commonly defined by biotite alignment in felsic volcanic rocks and also by brittle fractures. Spacing of the S_2 cleavage ranges from a few centimetres up to several tens of centimetres (Fig. 11b, c). Locally, S_2 kink bands are common features in volcaniclastic rocks (Fig. 11b). In general, the dominate NE trend of S_1 mimics the orientation of a NE–SW-striking high-strain zone hosting the Tjårrojåkka Cu–Au deposit (cf. Edfelt et al., 2005, 2006).

5.4   Kaitum West area

The Western Supracrustal Belt progressively widens southward toward the Kaitum West area (Figs. 2, 12). Overall, the bedrock is dominated by felsic to intermediate volcanic to volcaniclastic rocks with some additional basalt sequences. Structural observations indicate the area constitutes several low-strain zones that border a central high-strain block (Fig. 12). Most of the strain is apparently accommodated by relatively narrow shear zones transecting felsic volcaniclastic rocks in the central part of the area (Fig. 12). Locally to the west, highly strained basaltic and andesitic rocks do occur; however, these sequences generally show low strain intensity.

Bedding markers are rare in the Kaitum West area, and F1 folds were not recognized. Within the high-strain central block (Fig. 12), a polymict and poorly sorted clastic horizon occurs (Fig. 13a, b). This horizon contains a penetrative S_1 cleavage (266/79) defined by sericite + biotite + chlorite-dominated shear bands that trend subparallel to bedding and is particularly well developed at the margins of compositional layers (Fig. 13a). At the outcrop scale, the S_0/S_1 composite fabric is isoclinally folded (Fig. 13b) around a measured fold axis (335/60) plunging moderately to the NW. Locally, a S_1 high-strain cleavage is transposed into later shear bands (possibly S_2) that parallel the main shear zone system (Fig. 13c, d). This indicates relatively high ductile strain was localized both during D_1 and D_2 in the Kaitum West area.

The easternmost low-strain block is affected by F_2 folding around a calculated β axis plunging steeply to moderately towards the south (β: 182/67; Fig. 12). Within the cen-

tral high-strain block, several NW–SE-, N–S-, and locally E–W-trending high-strain zones and shear zones are present (Fig. 12). We interpret the central high-strain block as the northern continuation of the shear zone system mapped in the Fjällåsen–Allavaara area (see Sect. 5.5).

Kinematic indicators in the Kaitum West area suggest southwest-side-up and shallow to steep oblique dextral displacement that is associated with a south-plunging stretching lineation. This interpretation is based on SCC′ fabrics and a asymmetric quartz sigmoid with stair-stepped pressure shadows (Fig. 13e). The same sense of shear is indicated by a sinistral SC fabric (Fig. 13f) observed along a north-plunging stretching lineation north of the Kaitum West area (south of Ekströmsberg; Figs. 2, 3) where the same shear zone system is related to a major fold structure (Fig. 12). Locally, a contradicting sense of shear (east block up) is indicated by asymmetric sigma clasts with poorly developed pressure shadows.

5.5   Fjällåsen–Allavaara area

The area between Fjällåsen and Allavaara is dominated by felsic, intermediate, and mafic volcanic and volcaniclastic rocks. The dominant structural grain is an approximately N–S-trending set of high-strain zones (Fig. 14) associated with a well-developed N–S-trending penetrative foliation. The foliation is defined by the alignment of strained amphibole, biotite, feldspar, quartz, and locally magnetite (Fig. 15a) and is here designated S_1. Bedding is locally observable as compositional layering in volcanosedimentary rocks and is typically subparallel to the S_1 foliation. Locally, isoclinally F_1-folded quartz and amphibole veins and bedding can be observed (Fig. 15b, c). Shearing is common and localized in prominent high-strain zones that transpose S_0 and S_1 and form distinct mylonites (Fig. 15d). S_0 and S_1 are folded openly to tightly into meso- and macro-scale F_2 folds (Fig. 15e, f). An axial surface parallel cleavage (S_2) is locally observable as a weakly developed, brittle, spaced cleavage (Fig. 15e, f). Locally, this S_2 cleavage shows en echelon fracturing (Fig. 15b). Mineral lineations variably plunge steeply to moderately towards the north and south. Based on asymmetric sigma clasts and SC fabrics, a reverse west-block-up sense of shear is interpreted for the majority of deformation zones in this area. The central shear zone in Fjällåsen hosts the Fjällåsen Cu prospect and shows oblique kinematics with a reverse west-block-up and sinistral sense of shear along a mineral lineation plunging 60° N (Fig. 14).

5.6   Metamorphism and hydrothermal alteration along the WSB

Mineral alteration associations identified along the WSB based on mineralogical, textural, crosscutting, and/or over-printing relationships are presented in this section. Although several associations likely formed in response to a progressively evolving and likely protracted hydrothermal system(s),
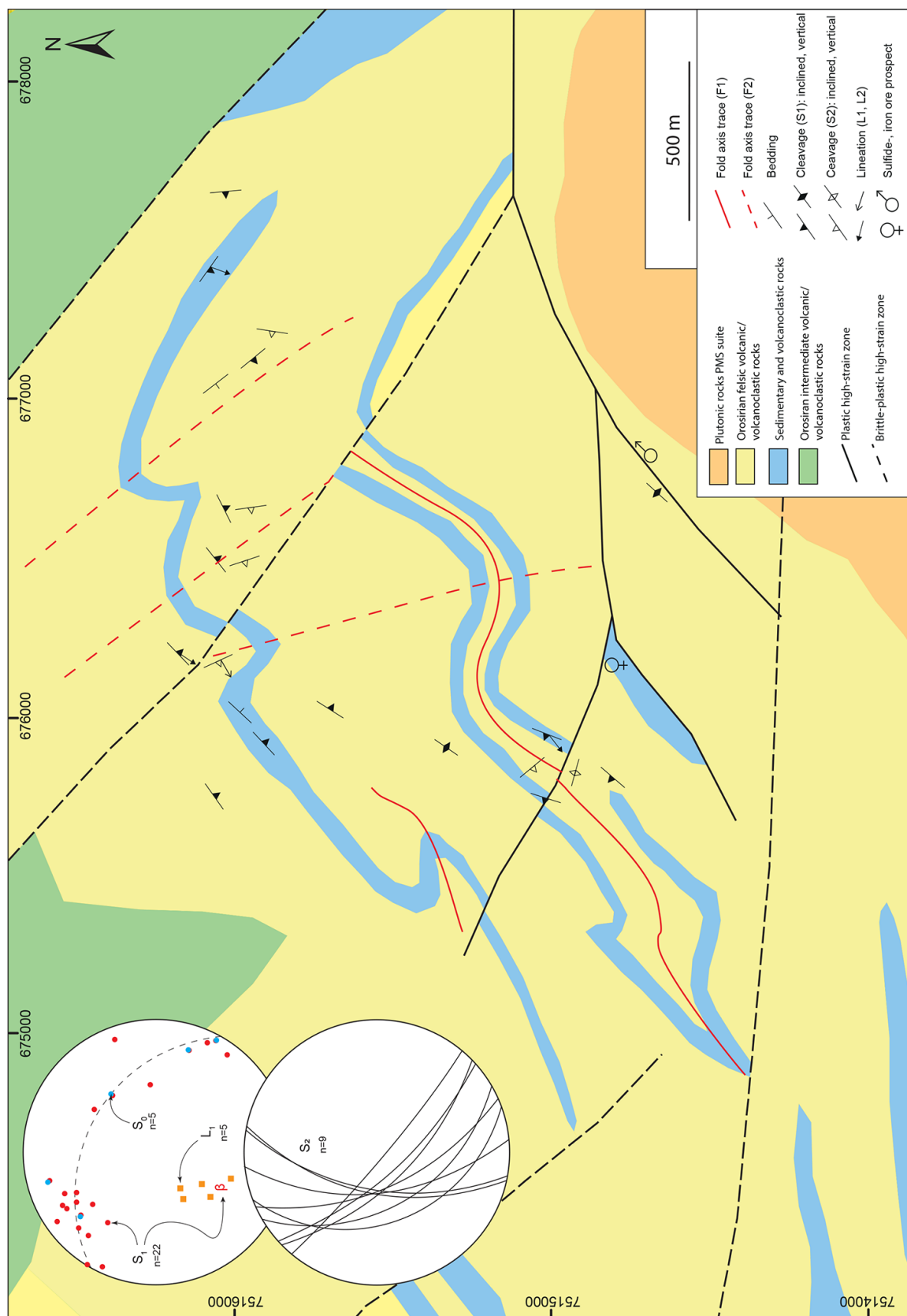
Figure 10. Geological map of the Tjårrojåkka key area. Modified after Offerberg (1967). Coordinates: Sweref99.
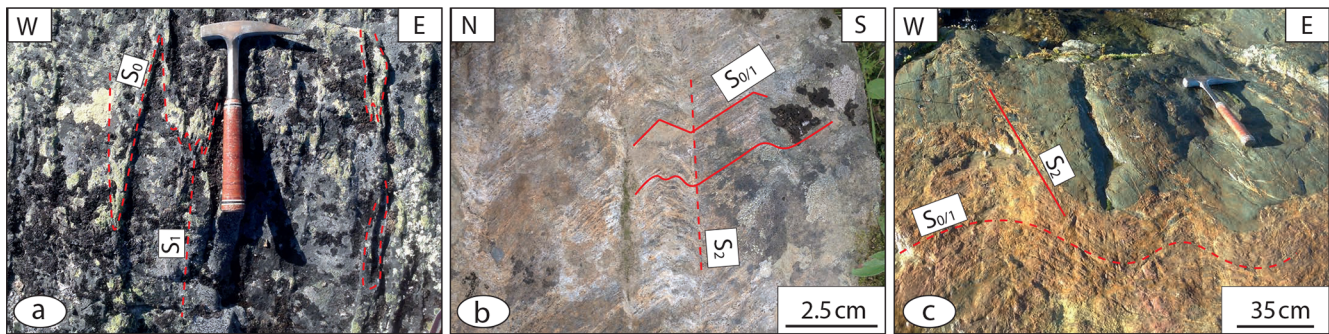
Figure 11. Field images of key localities in the Tjårrojåkka key area. **(a)** Isoclinal F_1 folding, X675916 Y7515915. **(b)** Open chevron-style F_2 folding with spaced S_2, X676285 Y7516107. **(c)** Open concentric F_2 folding with spaced S_2, X675985 Y7516176. Coordinates: Sweref99.

the new alteration mapping results provide a field-based classification/paragenetic scheme for the various alteration occurrences.

An epidote + plagioclase + hornblende association occurs parallel to S_1 fabrics in mafic volcanic rocks in the Ekströmsberg area and forms a moderately intense and pervasive metamorphic mineral association (Fig. 16a). Additionally, veins hosting hornblende + epidote locally occur and preserve internal foliations that are laterally consistent with S_1 fabrics in adjacent wall rocks (Fig. 16a), suggesting a relatively early timing (i.e. pre- to syn-D_1). However, hornblende shows syntectonic growth (Fig. 16b, c), and the S_1 foliation can be continuously traced within the matrix and as a preserved S_1 in the hornblende, indicating that the vein mineralogy was altered during prograde metamorphism approximately broadly coincident with D_1. In the Eustiljåkk area (Figs. 2, 5), epidote commonly developed as a retrograde product replacing disseminated hornblende porphyroblasts, indicating retrograde metamorphic processes affected the area.

Scapolite ± albite hydrothermal alteration overprints pervasive magnetite + amphibole alteration of basaltic rocks in the Kaitum West area. However, scapolite ± albite alteration is also locally overprinted by irregular and patchy amphibole + magnetite zones that tend to be developed along S_1 foliations (Fig. 17a). Thus, both associations are interpreted to be broadly coeval and formed during D_1. Discordant magnetite + amphibole veins with white to buff albite haloes occur locally in basaltic rocks with low strain intensities (Fig. 17b) and are affected by more pervasive (disseminated) magnetite + amphibole alteration.

In general, scapolite ± albite alteration is common throughout the WSB and is mainly observed in compositionally mafic rocks (i.e. basalt and dolerite) as a distinctive speckled (porphyroblastic) pale-grey to creamy-white granular discolouration on exposed surfaces (Fig. 17c). Disseminated scapolite porphyroblasts are typically medium- to coarse-grained (1–8 mm) and irregular tabular to elongated prismatic, and represent ca. 10–35 vol % of altered rock units (Fig. 17c). Weakly to strongly developed porphyroblas-

tic scapolite ± albite alteration is best preserved in relatively low-strain areas adjacent to or within NNW- to N-trending shear zones. In the Eustiljåkk area (Figs. 2, 3), porphyroblastic scapolite alteration affects mafic dykes in zones with relatively high strain, while it locally overprints inferred S_0 bedding planes in basalt units in the Ekströmsberg area (Figs. 2, 3, 8b). Discordant, vein-hosted scapolite ± albite alteration is widespread in the Vieto area (Figs. 2, 3). These veins are affected by shearing with a probable D_2 timing (Fig. 17d); hence, the veins are interpreted as being formed pre-D_2.

Deformed and discordant calcite veins are common throughout the WSB and are mainly present in low-strain blocks dominated by mafic rocks. However, pronounced calcite alteration also shows syn- to post-D_2 timing since it overprints clear S_2 shear zone fabrics in high-strain zones. Syn-tectonic (D_2) calcite associated with sparse occurrences of sulfide (pyrite + chalcopyrite) overprints relatively intense and pervasive tremolite–actinolite alteration (Fig. 17e) at one locality in the northern part of the Ekströmsberg area where it forms part of an amphibolitic L tectonite within a steep, reverse dip-slip shear zone that transects mafic rocks (Fig. 9a). Intense and pervasive calcite alteration shows a post-D_2 timing in the nearby Vieto area (Figs. 2, 3), where relatively undeformed calcite overprints an S_2 fabric in a moderately (ca. 285/75) west-dipping shear zone intersecting Rhyacian basalt (Fig. 17f).

Hydrothermal mineral associations restricted to D_2 structures are in general potassic–ferroan in character comprising K-feldspar, quartz, and epidote associated with Fe oxide and sulfide. The most prominent alteration association in the Tjårrojåkka area is a relatively intense and pervasive K-feldspar + epidote + quartz hydrothermal alteration association that overprints S_1 foliation. Locally, both K-feldspar and epidote appear to be remobilized into S_2 spaced cleavage domains as well as volcanosedimentary bedding (Fig. 17g). In the Kaitum West area, a relatively intense, selectively pervasive epidote + K-feldspar association is spatially related to localized Cu-sulfide weathering and overprints a weak, pervasive amphibole + magnetite alteration in a mafic
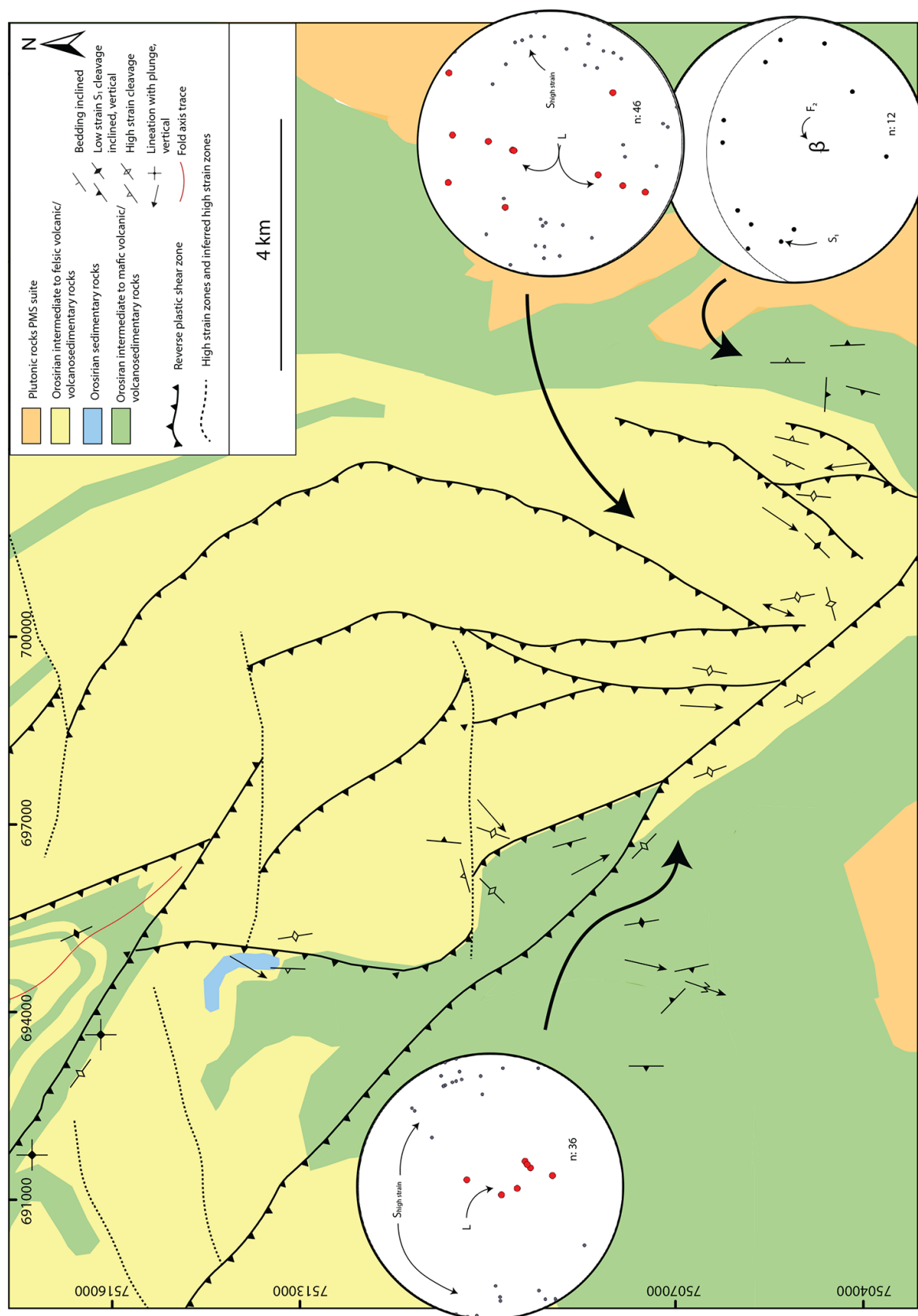
Figure 12. Geological map of the Kaitum West key area. Modified after Offerberg (1967). Coordinates: Sweref99.
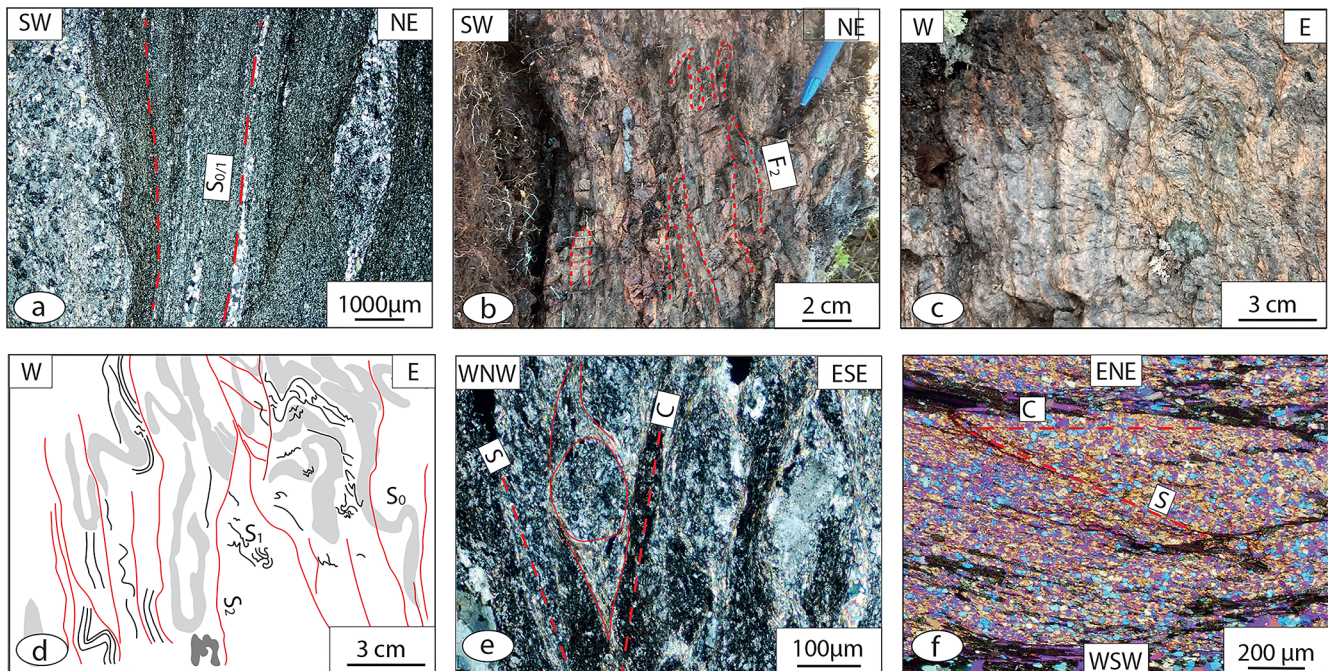
Figure 13. Thin-section photographs and field images/sketches of key localities in the Kaitum West key area. **(a)** Micrograph of S_0/S_1 composite fabric in volcanosedimentary rock, X698952 Y7505460. **(b)** Isoclinal mesoscale folding of the S_0/S_1 fabric **(a)**. **(c)** Volcanosedimentary unit showing a high-strain cleavage subparallel to S_0. The S_0/S_1 fabric is transposed into the direction of D_2 shear bands, X700402 Y7504830. **(d)** Simplified sketch of **(c)**. **(e)** SC fabric and asymmetric dextral sigma-sigmoid viewed along shallow south-plunging stretching lineation, X702488 Y7504983. **(f)** SC fabric indicating sinistral kinematics viewed along steep, north-northwest-plunging stretching lineation, X693703 Y7519820. Coordinates: Sweref99.

volcanic rock (Fig. 17h). In the Ekströmsberg area, a relatively intense, shear-band-hosted biotite + magnetite + K-feldspar + muscovite association affects a rhyodacitic volcanosedimentary rock intersected by steep, approximately E–W-trending sinistral strike-slip shear zones with a D_2 timing (Fig. 17k, l). The biotite-bearing shear bands are oriented subparallel with the volcanosedimentary bedding (S_0).

Selectively pervasive K-feldspar alteration (replacing albite) is common in intermediate to felsic volcanic rocks throughout the WSB (Fig. 17k) and is typically accompanied by weak retrograde sericite and hematite staining of secondary K-feldspar as well as epidote. K-feldspar alteration of albite of this type is the only hydrothermal alteration with a syn- to post-D_2 timing that is pervasive over large distances and not directly associated with tectonic structures.

The paragenetically latest hydrothermal mineral alteration identified in this study constitutes epidote forming patches on fracture planes intersecting selectively pervasive K-feldspar alteration at Tjårrojåkka. This association produces a distinctive reddish-green rock (Fig. 17l) with a late timing relative to brittle deformation (veins and fractures) of uncertain timing.

The hydrothermal mineral alteration associations identified in this study are summarized as a simplified alteration map in Fig. 18. The map shows that magnetite + amphibole

alteration is spatially correlated to scapolite ± albite alteration, with the latter affecting large areas at some distance from dominant structures. The intensity of the potassic alteration seems to decrease towards the north and increases towards the south, where ca. 1.8 Ga granites are found. The uncertainty of the map is relatively high due to the generally low rock exposure of the WSB.

Overall, the identified metamorphic and hydrothermal mineral associations are summarized as follows:

- D_1-related fluid flow (or marginally later):

  - regional epidote–amphibolite facies metamorphism, early to syn-D_1;
  - regionally pervasive amphibole + magnetite alteration, early to syn-D_1;
  - discordant, vein-related amphibole + magnetite + albite alteration, early to syn-D_1;
  - selectively pervasive scapolite ± albite alteration or growth of albite–scapolite porphyroblasts along S_0 and S_1 structures, syn- to late D_1;
  - shear-zone-hosted (selectively pervasive) actinolite + tremolite alteration, late D_1;
  - calcite in veins with an uncertain temporal relationship to D_1, but probably pre-D_2;
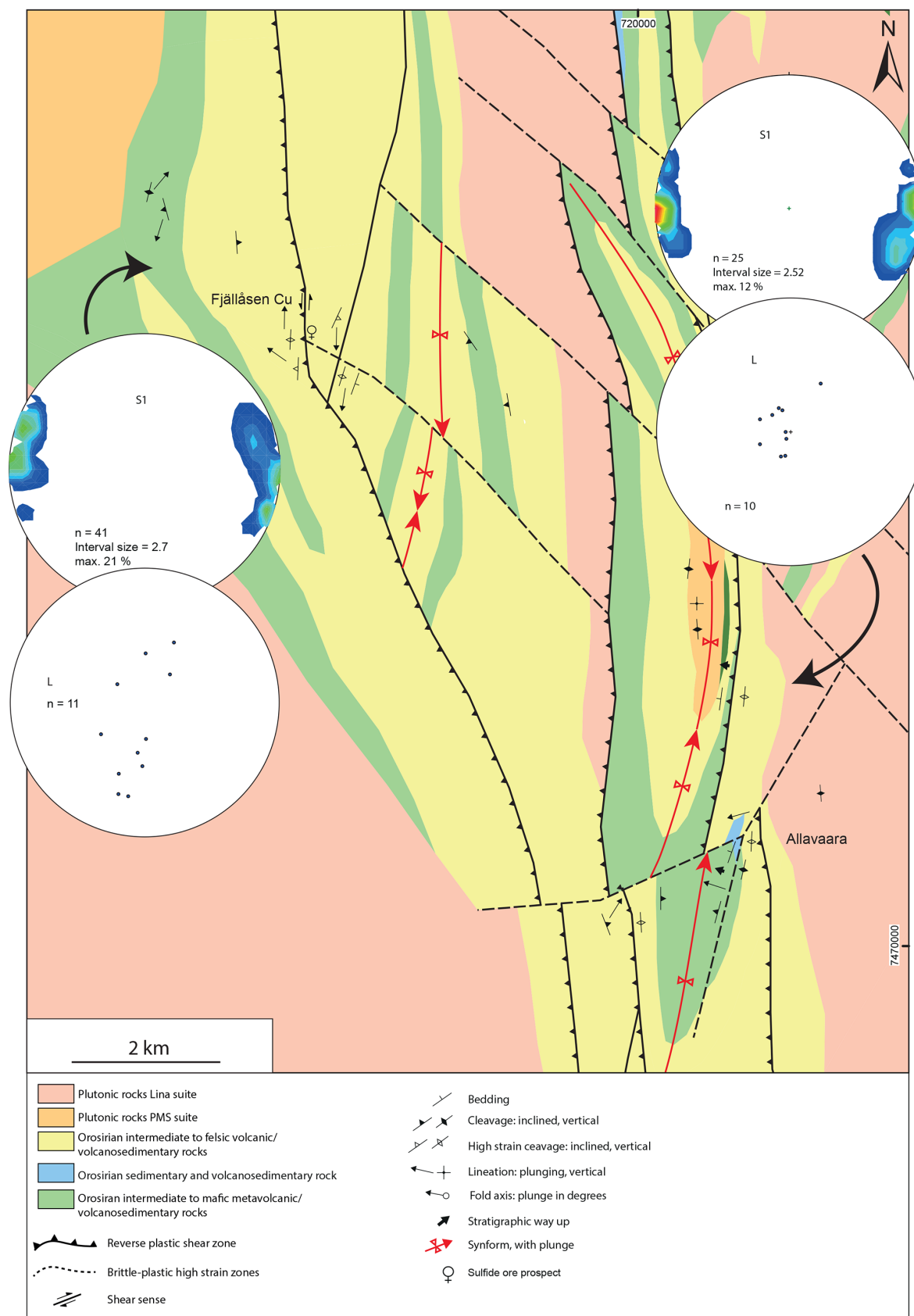
Figure 14. Geological map of the Fjällåsen–Allavaara key area. Modified after Witschard (1975). Coordinates: Sweref99.
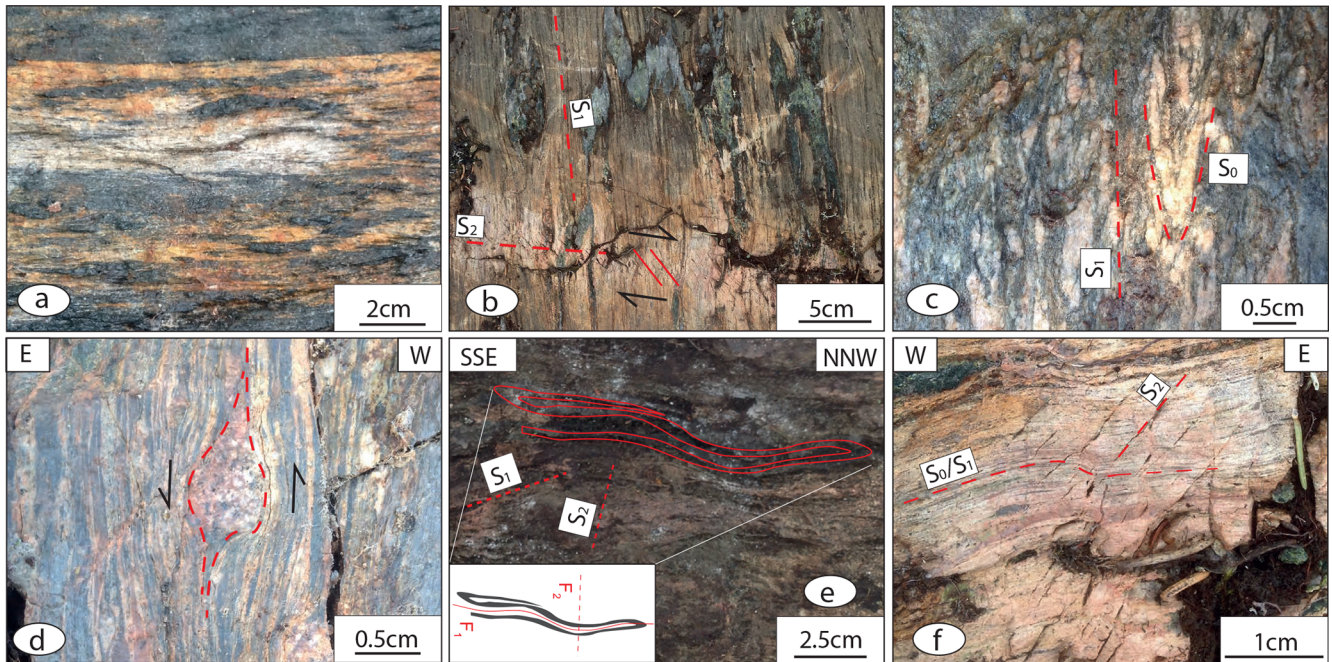
Figure 15. Field images of characteristics of the Fjällåsen–Allavaara key area. **(a)** High-intensity foliation, X721253 Y7473543. **(b)** Isoclinally folded quartz and amphibole veins with related axial planar S_1 cleavage. Brittle-plastic S_2 with dextral sense of shear, X721192 Y7473733. **(c)** Tight F_1 folding of S_0, X714642 Y7479559. **(d)** Asymmetric lithic sigma clast viewed along steep, north-plunging stretching lineation, X715483 Y7478182. **(e)** Isoclinal F_1 gently refolded by F_2, X713553 Y7480026. **(f)** Gentle F_2 folding of S_0/S_1 with associated brittle-plastic S_2, X721194 Y7473733. Coordinates: Sweref99.
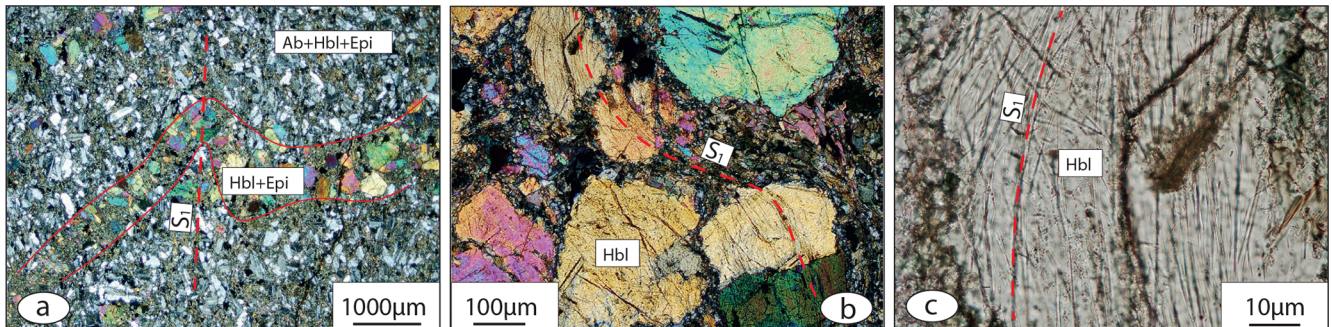
Figure 16. (a) Albite + hornblende + epidote metamorphic fabric aligned with axial planar S_1. Folded vein hosting hornblende + epidote. **(b)** Syn-tectonic growth of hornblende. **(c)** Needle-shaped mineral forming traces of S_1 in hornblende. All images from X690267 Y7529944, Ekströmsberg. Coordinates in Sweref99. Hbl: hornblende; Ab: albite; Epi: epidote.

– scapolite in veins with an uncertain temporal relationship to D_1, but probably pre-D_2.

– D_2-related fluid flow (or marginally later):

  – local S_2 shear-band-filling biotite + magnetite + K-feldspar + muscovite alteration, syn-D_2;

  – local vein-related K-feldspar + epidote + iron oxide ± sulfide alteration, syn-D_2;

  – regionally distributed, patchy (selectively pervasive) K-feldspar alteration of plagioclase, syn- to post-D_2;

– shear-zone-hosted calcite alteration, syn- and late/post-D_2;

– local fracture-filling and patchy epidote alteration, post-D_2;

– retrograde sericite alteration, post-D_2.
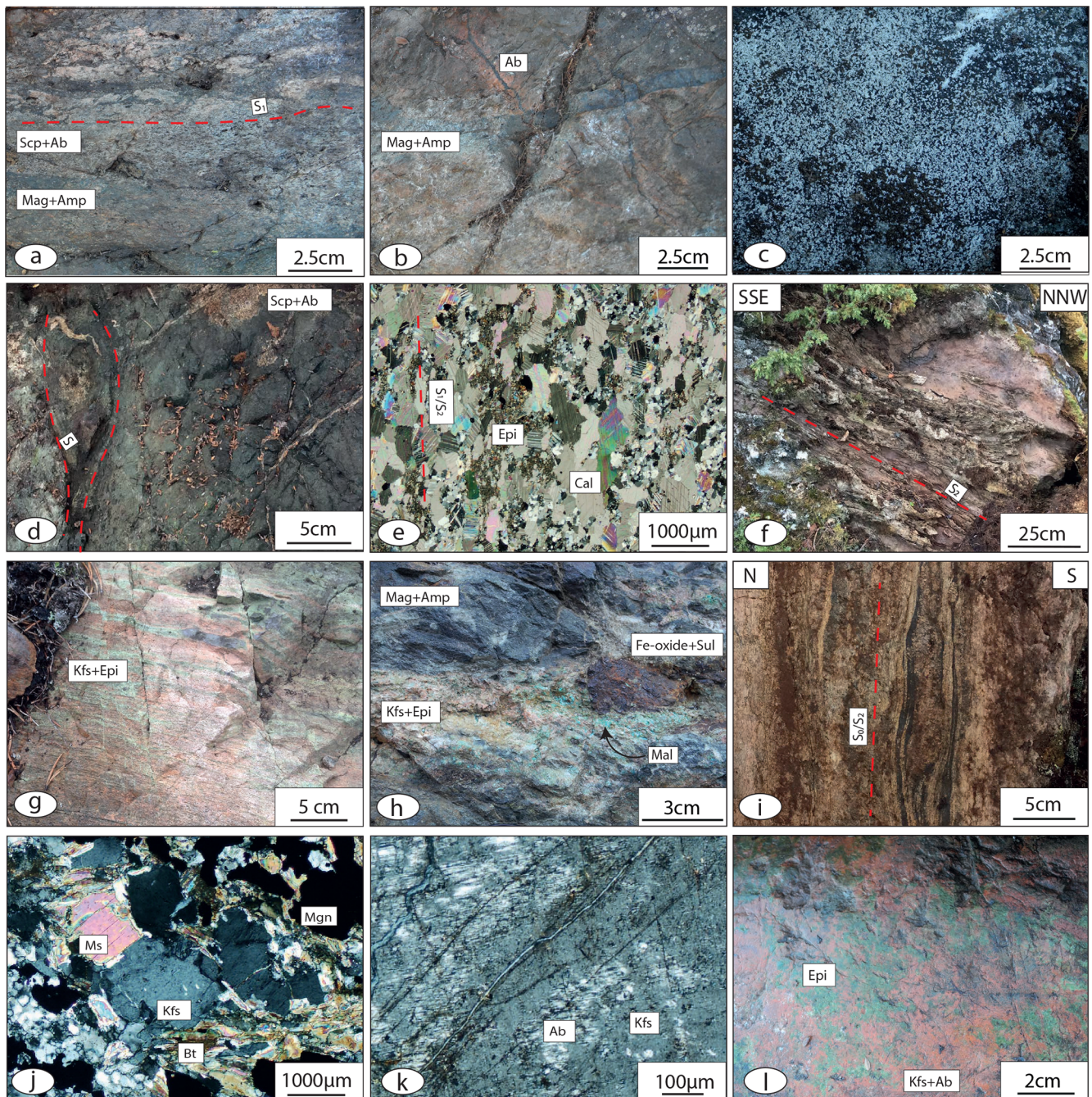
Figure 17. Thin-section and field images of alteration styles throughout the WSB. **(a)** Scapolite + albite overprinting magnetite + amphibole, X695488 Y7507194, Kaitum West. **(b)** Vein-hosted magnetite + amphibole with reddish albite haloes, X695459 Y7507412, Kaitum West. **(c)** Scapolite porphyroblasts, X696049 Y7507684, Kaitum West. **(d)** Scapolite in veins and patches transposed by later shear bands, X697177 Y7532766, Vieto (see Fig. 2). **(e)** Calcite overprinting actinolite–tremolite in L tectonite in Fig. 9a. Calcite aligned with S_1/S_2 with unde-formed granular epidote at grain boundaries, X689886 Y7530423, Ekströmsberg. **(f)** Reddish calcite overprinting ductile shear zone fabrics, X698369 Y7534383, Vieto (see Fig. 2). **(g)** K-feldspar + epidote concentrated along volcanosedimentary bedding X721289 Y7471362, Fjällåsen–Allavaara. **(h)** K-feldspar + epidote + Fe-oxide + sulfide + malachite overprinting pervasive magnetite + amphibole, X694578 Y7506821, Kaitum West. **(i)** E–W-directed D_2 shear zone with magnetite bands, X690231 Y7527374, Ekströmsberg. **(j)** Shear-band-hosted biotite + magnetite + quartz + K-feldspar + muscovite from the locality in **(l)**, Ekströmsberg. **(k)** Selectively pervasive K-feldspar replacing albite in same outcrop as Fig. 9c, X691491 Y7527635, Ekströmsberg. **(l)** Selectively pervasive K-feldspar alteration overprinted by epi-dote on a fracture plane, X696619 Y7508353, Kaitum West. Coordinates in Sweref99. Scp: scapolite; Ab: albite; Mag: magnetite; Amp: amphibole; Epi: epidote; Cal: calcite; Kfs: K-feldspar; Sul: sulfide; Mus: muscovite; Bt: biotite.
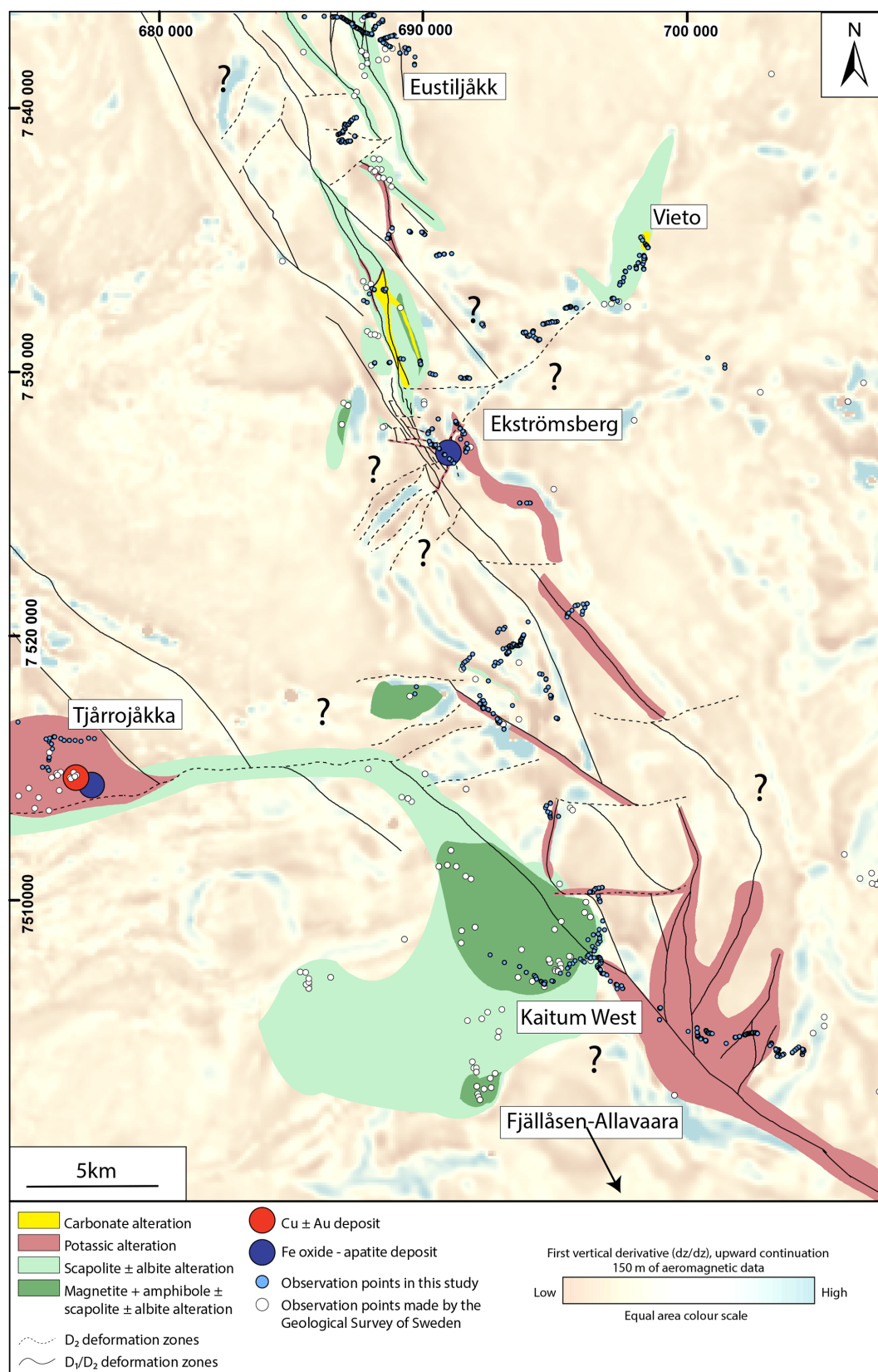
Figure 18. Geological map showing the spatial distribution of identified hydrothermal mineral associations and their relation to dominant structures and aeromagnetic anomalies. The map is based on the observations performed in this study together with a compiled database of recorded alteration minerals at the Geological Survey of Sweden. Coordinates in Sweref99.

6   Discussion

6.1   Structural evolution of the WSB

In general, the structural elements preserved within the WSB are consistent with a complex, polyphase deformation history. Locally, S_1 cleavages are axial planar to F_1 folds affecting S_0 bedding planes and magmatic flow structures associated with sedimentary, volcanosedimentary, or volcanic rocks. Overall, F_1 folds are generally poorly exposed and are thus difficult to constrain due to the lack of clear bedding and/or stratigraphic way-up indicators. Where observed, however, F_1 folds are tight to isoclinal and are either upright or overturned, with the latter verging eastward (Figs. 5, 7). F_1 folds in the southern Ekströmsberg area (Fig. 8) have a relatively steep calculated β axis that plunges towards the SSW (β: 195/75), which is a typical feature for F_2 folds throughout the WSB and suggests some F_1-fold axes were rotated into a steep southward plunge during D_2 transposition.

S_1 cleavages throughout the WSB are best preserved in relatively low-strain domains as a penetrative planar fabric in supracrustal rocks, while they are only weakly developed in adjacent shoshonitic plutonic rocks (i.e. Perthite monzonite suite intrusions; see Fig. 4). We interpret the relative timing of the shoshonitic (PMS, perthite monzonite suite) plutonic rocks as syn- to late D_1. Reported igneous ages for shoshonitic (PMS) plutonic rocks across northern Norrbotten range from ca. 1.88 to 1.86 Ga (Bergman et al., 2001; Sarlus et al., 2017; Kathol and Hellström, 2018). Thus, we interpret the absolute timing of syn- to late-D_1 deformation that affected the WSB to the later ages of the same time span, i.e. 1.88–1.86 Ga.

Mylonitization of volcanic-sedimentary rocks along the WSB frequently shows subparallel orientations to the regionally extensive and laterally continuous S_1 cleavage. Although the level of exposure does not allow for accurate estimations of the width of these zones, our mapping experience combined with ground magnetic signatures in the Ekströmsberg area (Frietsch et al., 1974) indicates that these zones are relatively thin (metres to tens of metres), controlled by lithological contrasts (or primary depositional features), and display sharp contacts to adjacent lower-strain rocks. Overall, the mylonitic strain appears to be favourably partitioned by volcaniclastic and sedimentary horizons that are sandwiched between more competent volcanic rocks throughout the WSB.

Penetrative fabrics formed during D_1 temporally coincide with the metamorphic peak indicated by syn-tectonic growth of hornblende in the Ekströmsberg area (Fig. 16b), implying temperatures > 450 °C (e.g. Blatt et al., 2006). In comparison, similar temperature conditions are suggested by GBM (grain boundary migration)-SGR dynamic quartz recrystallization textures observed in the Kaitum West area indicating temperatures of ca. 500 °C (Passchier and Trouw, 2005). However, dynamic quartz recrystallization textures (SGR with minor BLG) observed in D_1 shear zones suggest lower syn-deformation temperatures of ca. 400 °C (Fig. 9f). This may indicate that shear zone activity during D_1 postdates the metamorphic peak and that non-coaxial strain dominated the deformation during the late stages of D_1.

In general, S_2 cleavages developed predominantly in NNW–SSE- and approximately E–W-trending high-strain zones. Where S_1 is not completely transposed into S_2 parallelism or overprinted by high-strain S_2 fabrics, the S_1 cleavage is locally overprinted by a S_2 crenulation cleavage (cf. Fig. 9e). Dynamic quartz recrystallization textures formed during D_2 in the mylonite zones (SGR texture with minor BLG) suggest ambient temperatures of ca. 400 °C; however, brittle feldspar observed in association with SGR quartz textures (Fig. 9i) in an E–W-trending mylonite indicates the temperature as slightly lower (< 400 °C) in the E–W-trending structures during D_2 (Passchier and Trouw, 2005).

In low-strain blocks throughout the WSB, S_1 planar structures are folded into meso- to macro-scale F_2 folds with fold axes generally plunging moderately to steeply (60–80°) northward or southward (Figs. 5, 10, 11, 12, 13). Axial planar S_2 cleavage related to the F_2 folds in the low-strain blocks are rare. Only a few examples in the Tjårrojåkka and Fjällåsen areas as well as north of the Ekströmsberg area have been observed as axial planar, brittle, spaced cleavages (Figs. 11b, c, 15e). This characteristic of D_2 deformation is typical for this part of Norrbotten and is also observed east of the WSB. For example, in the Gällivare area (Fig. 1), Bauer et al. (2018) report folding of an S_1 gneissic fabric into F_2 synformal structures without axial planar S_2 cleavage. In the Aitik Cu–Au–Ag deposit also near Gällivare (Fig. 1), Wanhainen et al. (2005, 2012) report lower amphibolite facies metamorphism and deformation at 500–600° and 4–5 kbar between ca. 1.89 and 1.87 Ga. This medium-grade tectonothermal event was later overprinted by a hydrothermal event estimated at 200–500 °C and 1–2 kbar at ca. 1.78 Ga based on fluid inclusion data and geochronology (Wanhainen et al., 2012). The findings in the Aitik Cu–Au–Ag and Malmberget IOA deposits may not be directly applicable to the WSB in terms of metamorphic-hydrothermal PT conditions but are compatible with a more intense earlier deformation event (regional D_1) overprinted by a weaker deformational event (regional D_2), which we suggest represents the overall regional deformation history.

While the identification of two generations of planar fabrics is relatively straightforward in the WSB based on their orientation and interrelationships, linear structures are more difficult to interpret due to the lack of crosscutting relationships. Crenulation of mylonitic cleavage has only been observed along near-vertical stretching lineation, which leads us to interpret the well-clustered near-vertical stretching lineation in Fig. 20 as L_2. The sense of shear associated with subvertical L_2 lineation is reverse dip-slip (Fig. 9g) and is best explained by an E–W compressional stress field. Sinistral strike-slip movement along steep, approximately E–W-trending shear planes (Fig. 20b) offsetting the NNW–

SSE-trending structural grain in the Ekströmsberg area are D_2 structures, and the associated shallowly east-plunging stretching lineation is designated as L_2. Stretching lineations measured on S_1 planes in low-strain blocks are interpreted to be L_1 structures. The orientation of L_1 lineation varies considerably more than that of stretching lineation measured in relatively high-strain zones (cf. Fig. 20a–b). We suggest that the non-clustered shallowly to moderately north- and south-plunging stretching lineation (Fig. 20b) of the NNW–SSE-trending mylonites might represent traces of L_1 lineation. The sense of shear associated with the inferred L_1 lineation is reverse oblique slip with the SW side up and best explained as resulting from NE–SW-directed crustal shortening. This implies that the kinematics of D_1 and D_2 are best explained by two compressional events that deviate approximately 45° from each other. Based on the assumption that traces of L_1 can be identified, we argue that the steep to near-vertical cluster in the low-strain L_1 plot (Fig. 20a) represents L_1 lineation that was subsequently transposed during D_2 in a similar manner to how F_1-fold axes were transposed in the Ekströmsberg area.

The NNW–SSE-trending mylonites with moderately plunging stretching lineation (L_1) suggest oblique-slip SW-side-up kinematics based on SCC′ fabrics and rotated porphyroclasts in oriented samples from the Ekströmsberg, Kaitum West, and Fjällåsen–Allavaara key areas. These kinematic indicators suggest that both sinistral and dextral movements occurred, with dextral sense of shear observed along moderately S-plunging lineation (Fig. 13e) and sinistral sense of shear observed along moderately N-plunging lineation (Figs. 9f, 15d). Similar kinematics are indicated during D_1 by the east-verging F_1 fold in the Eustiljåkk area, implying consistent reverse oblique-slip southwest-side-up movement during D_1 throughout the WSB.

The kinematics derived from SC fabrics along the near-vertical lineations (L_2 generation) within the NNW–SSE-oriented mylonites in the Ekströmsberg and Fjällåsen areas indicate reverse dip-slip, W- to WSW-side-up sense of shear (Fig. 9g). This implies a reactivation of the NNW–SSE-trending structures during an approximately E–W-directed D_2 shortening. Additionally, sinistral strike-slip movement along E–W-trending shear zones in the Ekströmsberg area (Fig. 9h) indicate they were active during a ca. E–W compression coincident with reverse dip-slip movements along the NNW–SSE-trending mylonites. A late timing for the E–W-trending structures is supported by the consistent offset of NNW–SSE-trending grain by E–W-trending structures throughout the WSB (Fig. 3).

6.2 Summary of major deformation events affecting the WSB

Based on the new structural data presented in this paper and with reference to tectonic models proposed for surrounding areas (Wright, 1988; Talbot and Koyi, 1995; Bergman et al.,

2001; Angvik, 2014; Skyttä et al., 2012; Andersson et al., 2017; Sarlus et al., 2017; Grigull et al., 2018; Luth et al., 2018; Lynch et al., 2018b), we propose the following tectonic model that utilizes two major deformation events for the WSB (Fig. 21).

6.2.1 Pre-D_1 event

Syn-orogenic crustal thinning and mafic to felsic magmatism associated with back-arc basin development has been inferred for the wider WSB–Kiruna area based on regional petrological/geochemical studies (Perdahl and Frietsch, 1993; Martinsson, 2004; Sarlus et al., 2017, 2018). The Orosirian stratigraphic record in the central Kiruna area (Figs. 1, 4) represents one of the best-preserved conformable Svecofennian supracrustal sequences in northern Norrbotten and comprises rock types that are correlative with those within the WSB. This suggests basin development at Kiruna was coeval with the deposition of the supracrustal rocks dominating the WSB (Andersson, 2019). Based on this lithostratigraphic correlation, our deformation model for the WSB is predicated on the notion that the area initially developed within an extensional, basin-type setting that underwent subsequent compression and inversion.

6.2.2 D_1 event

NE–SW- to ESE–WNW-directed crustal shortening (this study; Wright, 1988; Talbot and Koyi, 1995; Lahtinen et al., 2005; Angvik, 2014) that was coeval with syn-tectonic plutonism at 1.88–1.86 Ga (Bergman et al., 2001; Sarlus et al., 2017; Kathol and Hellström, 2018) generated ENE-verging, tight to isoclinal F_1 folds with shallowly NNW-plunging fold axes. A WSW-dipping axial planar S_1 cleavage/foliation is locally associated with these F_1 folds in the WSB.

Oblique reverse dextral and sinistral shear zones with west-side-up sense of shear developed during D_1 and produced the dominant NNW–SSE-trending, undulating, magnetic lineaments that characterize the WSB (Fig. 3; Bergman et al., 2001). Deformation along these zones during D_1 is indicated by the presence of crenulated S_1 (Fig. 9e) and high-strain S_1 fabrics that are tightly folded by later D_2 structures (Fig. 13c–d). Strain partitioning appears to have been controlled by lithological contacts (or perhaps pre-existing discontinuities) as the highest strain is recorded by favourable, less competent lithologies such as volcanosedimentary rocks.

Based on the relatively steep dip of the NNW–SSE-aligned structural grain and the broadly alkaline character of the affected volcanic rocks (Perdahl and Frietsch, 1993; Bergman et al., 2001; Martinsson, 2004; Martinsson et al., 2016; Sarlus et al., 2017, 2019), we favour a model involving inversion of an evolving back-arc basin to account for D_1-related structures in the WSB. Back-arc basin inversion took place under epidote–amphibolite metamorphic facies conditions (this study; Ros, 1979; Edfelt et al., 2005)
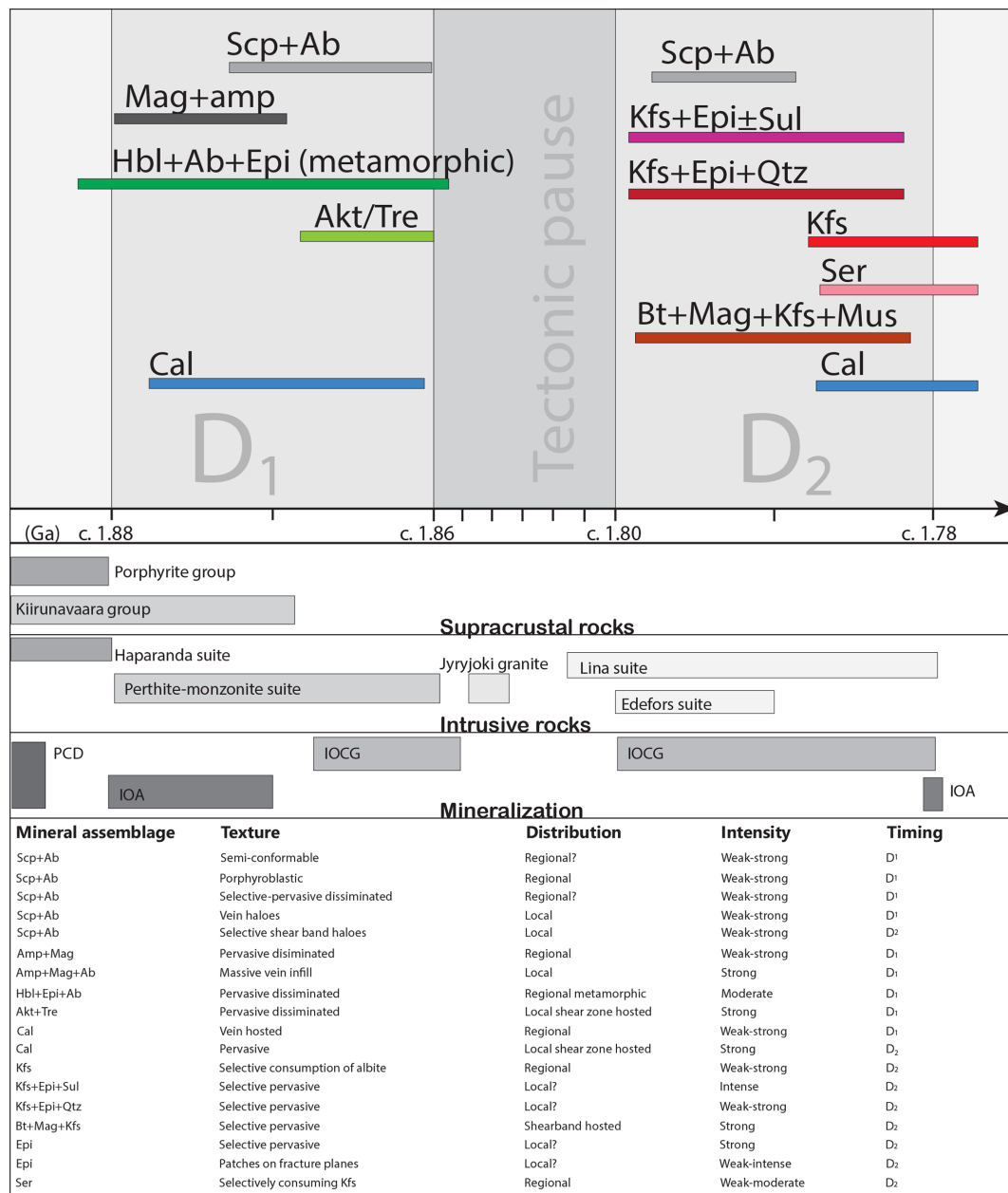
Figure 19. Summary of mineral alteration associations in the WSB and their inferred timings relative deformation. For comparison, the timing of supracrustal/intrusive rocks as well as mineralization in northern Norrbotten is included. Question mark indicates probable distribution.

as recorded by syn-tectonic growth of hornblende in albite + hornblende + epidote metamorphic textures in volumetrically minor Rhyacian pillow lavas in the Ekströmsberg area (Fig. 16a–c). This contrasts with models that envisage the development of a classic fold-and-thrust belt in the broader WSB–Kiruna area during D_1 (Wright, 1988; Talbot and Koyi, 1995). Consistent evidence for the rotation of originally shallow-dipping thrust-type structures into subvertical orientations was not found along the WSB. Furthermore, no classic fold–thrust belt features involving shallow thrusts and/or nappe stacks have been identified in nearby

areas (Vollmer et al., 1984; Wright, 1988; Talbot and Koyi, 1995; Grigull et al., 2018; Luth et al., 2018). However, Angvik (2014) identified a series of fold–thrust belts in the Rombak Tectonic Window, west of the WSB in Norway. It is possible that the Rombak Tectonic Window represents a fundamentally different setting and that the change from a classic fold–thrust belt to an extensional back-arc setting is to be found between the WSB and the Rombak Tectonic Window.
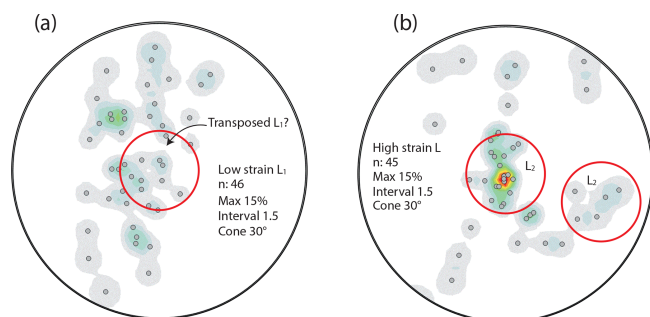
Figure 20. Lower-hemisphere equal-area stereographic projections of lineation throughout the WSB. Cones represent 30° circles. **(a)** L_1 stretching and mineral lineation measured on S_1 foliation planes in low-strain blocks. **(b)** Stretching and mineral lineation measured in high-strain zones.
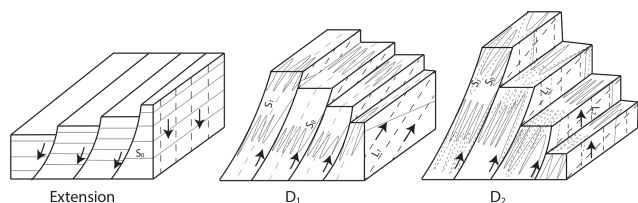
Figure 21. Conceptual model of the structural development of the WSB.

6.2.3　D_2 event

A phase of ca. E–W compression caused meso- to macro-scale folding of S_1 foliation and produced near-cylindrical, upright F_2 folds with steep, N- and S-plunging fold axes. Broadly similar F_2-fold characteristics are developed in all key areas throughout the WSB. Strong strain partitioning focused D_2 deformation into pre-existing NNW–SSE-trending oblique-slip D_1 shear zones, causing their reactivation with a reverse dip-slip, west-side-up sense of shear. Synchronously, near-vertical E–W-trending sinistral (and possibly dextral; Wright, 1988) brittle-plastic strike-slip shear zones were active and locally off set the NNW–SSE structural grain. Applying a basin inversion model to the WSB implies that the E–W-directed structures might have originated as transfer faults between NNW–SSE-trending normal faults and that the combined structural configuration was reactivated together, first during D_1 and later during D_2.

D_2-related kinematics are based on SC fabrics observed along steep to near-vertically plunging L_2 stretching lineations within NNW–SSE-trending high-strain zones at Ekströmsberg, north of Kaitum West and the Fjällåsen–Allavaara areas. Correlative microstructures are also observed within shallowly E-plunging stretching lineations in E–W-trending high-strain zones at the Ekströmsberg area. The E–W-directed offset of NNW–SSE-trending high-strain zones is interpreted from magnetic maps (Frietsch et al., 1974; Bergman et al., 2001). Joints and fracture planes pre-

date the latest epidote alteration in the area and are interpreted as developed either during D_2 or slightly thereafter.

6.3　Timing of D_1–D_2 deformation within the WSB, and comparative links with adjacent areas

Tectonic models for northern Norrbotten and the Skellefte district generally include an early phase of deformation at approximately 1.88–1.86 Ga (e.g. Wright, 1988; Talbot and Koyi, 1995; Lahtinen et al., 2005; Skyttä et al., 2012; Angvik, 2014). In the Skellefte district, the minimum timing of crustal shortening with related folding and shearing was constrained at 1874 ± 4 Ma (Skyttä et al., 2012), which is comparable to the maximum ages at 1888 ± 7 and 1865 ± 8 Ma for NNW–SSE-trending shear zones in the Kautokeino greenstone belt north of the WSB in Norway (Bingen et al., 2015). Similarly to this study's interpretation, Allen et al. (1996), Bauer et al. (2011), and Skyttä et al. (2012) proposed that shear zones in the Skellefte district formed during a phase of continental arc extension and volcanic activity prior to 1.88 Ga, and were subsequently reactivated ca. 1.87 Ga during accretion of the arc onto the Archean continent and subsequent crustal shortening.

In terms of later deformation events, Bauer et al. (2017) and Lynch et al. (2018b) report west-side-up movements during a D_2 phase of deformation in the Cu–Au-mineralized NDZ near Gällivare, which generated a duplex Riedel shear system within that composite zone. Additionally, Bauer et al. (2018) argue for E–W compression during a D_2 phase of deformation and link this event to the intrusion of syntectonic granites 1.8 Ga (e.g. Öhlander et al., 1987; Bergman et al., 2001; Sarlus et al., 2017). A similar timing of deformation is interpreted for the Rombak Tectonic Window ca. 100 km west of the WSB in Norway, where U–Pb zircon ages for syn-tectonic granites (Angvik, 2014) bracket the timing of a comparable deformation event between 1778 and 1798 Ma (D_3–D_4 in Angvik, 2014) . Based on the above studies, we suggest a similar timing for D_2 in this study, which includes folding, reverse dip-slip reactivation of NNW–SSE-trending D_1 shear zones, and strike-slip shearing along E–W-trending brittle-plastic structures (see Sect. 6.2 above).

6.4　Hydrothermal alteration, metamorphism, and their relationship to deformational events

A preferentially aligned hornblende + epidote + plagioclase mineral association defines S_1 continuous cleavages in mafic volcanic rocks in the Ekströmsberg area (Fig. 17g). A similar mineral association was used by Ros (1979) and Edfelt et al. (2005) to define the metamorphic grade affecting mafic rocks in the Tjårrojåkka area (Figs. 2, 3, 10). According to Spear (1993), hornblende + epidote + plagioclase would indicate a transition from greenschist to amphibolite facies metamorphic conditions. Similarly, we interpret

the hornblende + epidote + plagioclase association as a key metamorphic indicator mineral association (Ros, 1979; Edfelt et al., 2005), which accords with the generally accepted, but poorly constrained, low- to medium-grade low-P regional metamorphism of northern Norrbotten (e.g. Frietsch et al., 1997; Bergman et al., 2001; Skelton et al., 2018). In Fig. 16a, the hornblende + epidote + plagioclase S_1 fabric forms axial planes to a folded hornblende + epidote vein fill, which possibly indicates a pre-compressional timing for some hornblende + epidote and thus a pre-D_1 commencement of prograde metamorphism. However, hornblende in this vein displays syn-tectonic characteristics (Fig. 16b, c), implying that metamorphism probably peaked during the fabric-forming D_1 event.

Regional scapolite alteration in northern Norrbotten is thought to be linked to the formation of IOA and Cu–Au deposits there, having formed due to the activity of relatively high-salinity ore-forming fluids (Martinsson et al., 2016). In this respect, the widespread albite + scapolite alteration in the WSB may partly represent the effects of hydrothermal fluid flow associated with the formation of IOA and Cu–Au mineralization in the area. Several generations of albite + scapolite alteration are present throughout the WSB and in differing settings. For example, the porphyroblastic and the semi-conformable (selectively pervasive) types (Fig. 17a, c) are commonly encountered in low-strain blocks close to shear zones or in mafic dykes within or at the margins of metre-wide shear zones. Scapolite porphyroblasts are often undeformed and tend to overprint D_1 fabrics. Hence, we infer the timing of the regional porphyroblastic scapolite formation as syn- to late D_1. This inference is broadly consistent with metasomatic (titanite) U–Pb ages at 1851 ± 6 and 1850 ± 7 Ma reported for a scapolite-altered diorite east of the WSB (Martinsson et al., 2016). However, at the same locality, Smith et al. (2009) reported 1903 ± 8 Ma for scapolitization, which indicates that scapolite alteration in the Norrbotten area is likely polyphase and occurs as several generations.

Pervasive magnetite + amphibole alteration (Fig. 17a, h) is commonly distributed in the WSB, and it is locally overprinted and affected by S_1 foliation and interpreted as early to syn-D_1. Amphibole + magnetite alteration also occurs as discordant veins with albite haloes (Fig. 17b). The relative timing of these veins is difficult to resolve due to the lack of an association with other discernible tectonic structures, but we tentatively assign a D_1 timing and a paragenetic link with the pervasive amphibole + magnetite association based on their similar mineralogy and often close spatial relationship (see Fig. 19). Pervasive amphibole + magnetite occasionally shows an early timing relative to the early selectively pervasive albite + scapolite alteration (Fig. 17a). However, we have also observed the opposite relationship between pervasive magnetite + amphibole and early selectively pervasive albite + scapolite alteration. Thus, it is possible that both hydrothermal mineral associations represent an evolv-

ing calcic–sodic–ferroan alteration system similar to that suggested from other analogous IOA- and IOCG-mineralized terranes (e.g. Corriveau et al., 2016; Montreuil et al., 2016). However, in the WSB, a clear spatial zonation of hydrothermal alteration at the exposed surface has not been observed (e.g. Fig. 18), but it is possible that such a zonation is masked by overburden.

The hydrothermal mineral associations linked to D_2 in this study are potassic–ferroan in character and in most cases are hosted by D_2 structures. A late-D_2 timing is interpreted for the biotite + magnetite + K-feldspar + muscovite alteration hosted by sinistral E–W shear zones near the NNW–SSE-trending Ekströmsberg IOA deposit (Fig. 17k, l). A late-D_2 timing for this potassic–ferroan alteration is evident by offsetting relationships between the E–W structural grain and more dominant NNW–SSE-trending D_1 fabrics. Paragenetically late and structurally controlled potassic alteration associated with epidote occurs along volcanosedimentary bedding (Figs. 17g, 19) or as vein fills associated with iron oxides and sulfide crosscutting magnetite-amphibole alteration at the outcrop scale (Fig. 17h). In the Tjårrojåkka area, Edfelt et al. (2005) suggest K-feldspar alteration is paragenetically late relative to scapolite. Similarly, in the Gällivare area, K-feldspar alteration shows a late-D_2 timing and a close spatial relation to ca. 1.8 Ga granite and pegmatite (Bauer et al., 2018), hence in agreement with our observations from the WSB.

Locally, late-stage calcite associated with rare sulfide mineralization forms part of (Fig. 17e) or overprints (Fig. 17f) D_2 shear zone fabrics in structures intersecting mafic rocks. Late-stage carbonate deposition has been described for magnetite group IOCG in the Cloncurry district in Australia (Corriveau and Mumin, 2010) as well as in Norrbotten close to Kiruna (Fig. 1), where carbonates are associated with sulfides in a discordant albite-carbonate mylonite zone (Bergman et al., 2001). It is possible that the late-stage carbonate alteration reported in this study forms part of a larger ore-forming system during D_2. However, in the case where carbonate alteration overprints D_2 shear zone fabrics (Fig. 17f), the possibility that ingress of retrograde meteoric fluid depositing carbonate during downwelling as described by Kesler (2005) cannot be excluded at this stage of research.

Hydrothermal alteration with an inferred D_2 timing that does not show a direct association with tectonic structures is regional selectively pervasive (patchy) K-feldspar alteration (replacing albite), often accompanied by sericite and epidote. This is an important alteration component in the felsic volcanic rocks of the WSB (Fig. 17k), and it was documented already during the early mapping campaigns in the area (Offerberg, 1967). Few crosscutting relationships exists for this type of alteration; however, fracture planes carrying epidote (Fig. 17i) post-date this selectively pervasive K-feldspar alteration, implying the latter developed before brittle deformation, probably syn- to late D_2 and broadly coeval with the

structurally controlled potassic mineral associations occurring along the WSB.

The spatial distribution of identified hydrothermal mineral associations and their spatial correlation to dominant structures is summarized on the map in Fig. 18. The map shows that D_1-related mineral associations are confined to geological structures and also overprint areas distal to dominant D_1 structures. Overall, scapolite $\pm$ albite is more widespread than magnetite + amphibole alteration. The intensity of potassic alteration seems to decrease towards the north, which can be explained by the general absence of ca. 1.8 Ga granites in that part of the WSB. Carbonate alteration is confined to structures with an inferred D_2 timing. Distribution uncertainties for the alteration associations shown in Fig. 18 are high due to the scattered nature of the observations and the glacial till covering most of the WSB.

The alteration styles identified throughout the WSB may represent important vectors for both IOA and IOCG mineralization along the belt, in northern Norrbotten (e.g. Martinsson et al., 2016) and worldwide (e.g. Corriveau and Mumin, 2010). In our study, alteration styles typical for comparable IOA and IOCG districts elsewhere (i.e. calcic–sodic and potassic $\pm$ ferran associations) are consistently developed along the WSB and show a spatial association with certain generations of structures that can be correlated with the position of known IOA- and/or IOCG-style mineralization (e.g. the Ekströmsberg and Tjårrojåkka areas; Fig. 18).

Summary of hydrothermal alteration, metamorphism, and their relation to deformation

To summarize the relative timing of the various alteration styles and how they relate to Orosirian magmatism and mineralization in the WSB and northern Norrbotten in general, a summary sketch in Fig. 19 and the following key points are presented based on this study's results, combined with stratigraphic and geochronology data reported by Romer et al. (1994), Bergman et al. (2001), Wanhainen et al. (2005), Edfelt (2007), Smith et al. (2009), Westhues et al. (2016), Martinsson et al. (2016), Sarlus et al. (2017), and Bergman (2018):

- D_1:
  - emplacement of calc-alkaline intrusions (Haparanda suite) and coeval volcanic rocks (porphyrite group) as well as pre- to early D_1 in northern Norrbotten;
  - porphyry copper formation east of WSB, pre- to early D_1;
  - emplacement of mildly alkaline intrusions (Perthite monzonite suite) and coeval volcanic rocks (Kiirunavaara group), pre- to syn-D_1 in northern Norrbotten;
  - IOA mineralization east of the WSB (in central Kiruna) during pre- to early D_1;

- regional pervasive amphibole + magnetite alteration in the WSB, early to syn-D_1;
- discordant vein fill amphibole + magnetite + albite alteration, early to syn-D_1;
- metamorphic peak in the WSB (epidote–amphibolite facies metamorphism), syn-D_1 (earlier metamorphic onset as well as prolonged metamorphic conditions is possible);
- conformable albite–scapolite alteration or growth of albite–scapolite porphyroblasts in the WSB syn- to late D_1;
- IOCG mineralization east of WSB during late D_1;
- shear-zone-hosted pervasive actinolite + tremolite alteration, late D_1;
- calcite in veins with unknown temporal relation to D_1 but pre-D_2;
- scapolite in veins with unknown temporal relation to D_1 but pre-D_2.

- D_2:
  - emplacement of Lina and Edefors intrusive suites in northern Norrbotten, syn-D_2;
  - IOCG mineralization confined to shear zones east of the WSB, syn-D_2;
  - local shear-band-hosted biotite + magnetite + K-feldspar alteration in the WSB, syn-D_2;
  - local discordant vein-hosted K-feldspar + epidote + iron oxide + sulfide alteration, syn-D_2;
  - local discordant vein/shear band fill scapolite alteration, syn-D_2;
  - IOA and IOCG emplacement in the Tjårrojåkka area (WSB), late D_2;
  - calcite alteration, syn- and late to post-D_2;
  - regional selectively pervasive K-feldspar alteration, syn- to post-D_2;
  - local fracture-fill epidote alteration, post-D_2;
  - retrograde sericite alteration, post-D_2.

7 Conclusions

Based on the new structural mapping and microstructural investigation presented in this study, two major compressional events affecting the Western Supracrustal Belt in northwestern Norrbotten have been identified. These deformation events, D_1 and D_2, developed pronounced, corresponding structures which can be correlated with different types of mineral alteration associations within the belt. Shear zones

recording reverse oblique west-side-up kinematics were developed during D_1, giving rise to an undulating NNW-trending configuration of magnetic lineaments. D_1 produced a steep SW- to WSW-dipping, heterogeneously developed, penetrative, and continuous S_1 foliation related to F_1 folds with either tight, east-verging symmetry with a shallow NW-plunging fold axis or tight, upright symmetry with steep fold axes. Steep plunges of F_1-fold axes are interpreted to be a result of later D_2 transposition.

S_1 foliation was folded during D_2 into near-cylindrical F_2 folds with steep, N- and S-plunging fold axes. Axial planar S_2 foliations are rarely developed in relation to F_2 folds; where present, S_2 is a spaced cleavage on the centimetre to several-decimetre scale. The finite D_2 strain was partitioned into pre-existing D_1 shear zones, reactivating these structures with reverse dip-slip, west-side-up sense of shear. The D_2 strain was also partitioned into rheologically favourable lithotypes, such as volcanosedimentary rocks. Synchronously, E–W trending sinistral strike-slip shear zones were active and partly displaced earlier-formed NNW-trending structural grains.

D_1 is associated with regional scapolite $\pm$ albite alteration that is broadly coeval with regional magnetite $\pm$ amphibole alteration under epidote–amphibolite facies metamorphic conditions. The hydrothermal alteration that affected rocks during D_2 is generally structurally controlled and potassic $\pm$ ferroan in character and dominated by K-feldspar $\pm$ epidote $\pm$ quartz $\pm$ biotite $\pm$ magnetite $\pm$ sericite $\pm$ sulfides, as well as calcite. D_2 is also associated with selectively pervasive K-feldspar alteration replacing albite, affecting intermediate to felsic rocks without any direct spatial correlation to structures. This implies that our field-based observations support an early-D_1 timing for calcic–sodic alteration, whereas a later timing (syn-D_2) is interpreted for potassic $\pm$ ferroan alteration associations. In absolute terms, the timing of these fluid flow events may have differed by as much as ca. 80 million years based on previously reported geochronological data from northern Norrbotten.

References

Åhäll, K.-I. and Larsson, S.-Å.: Growth related 1.85–1.55 Ga magmatism in the Baltic Shield; a review addressing the tectonic characteristics of the Svecofennian, TIB-1, and Gothian events, GFF, 122, 193–206, 2000.

Allen, R. L., Weihed, P., and Svenson, S.-Å.: Setting of Zn-Cu-Au-Ag massive sulfide deposits in the evolution and facies architecture of a 1.9 Ga marine volcanic arc, Skellefte District, Sweden, Econ. Geol., 91, 1022–1053, 1996.

Andersson, J. B. H.: Structural evolution of two ore-bearing metasupracrustal belts in the Kiruna area, northwestern Fennoscandian shield, Licentiate thesis, Luleå University of Technology, Sweden, 28 pp., 2019.

Andersson, J. B. H., Bauer, T. E., Martinsson, O., and Wanhainen, C.: The tectonic overprint on the Per Geijer apatite iron ores in Kiruna, northern Sweden, Proceedings of the 14th SGA Biennal Meeting, 20–23 August 2017, Quebec City, Canada, 903–907, 2017.

Andersson, U. B.: Granitoid episodes and mafic-felsic magma interaction in the Svecofennian of the Fennoscandian Shield, with main emphasis on the $\sim$ 1.8 Ga plutonics, Precambrian Res., 51, 127–149, 1991.

Andersson, U. B., Neymark, L. A., and Billström, K.: Petrogenesis of Mesoproterozoic (Subjotnian) rapakivi complexes of central Sweden: implications from U-Pb zircon ages, Nd, Sr, and Pb isotopes, T. RSE Earth, 92, 201–228, 2002.

Angvik, T. L.: Structural development and metallogenesis of Paleoproterozoic volcano-sedimentary rocks of the Rombak Tectonic Window, PhD thesis, University of Tromsø, Norway, 284 pp., 2014.

Bauer, T. E., Skyttä, P., Allen, R. L., and Weihed, P.: Syn-extensional faulting controlling structural inversion- Insights from the Paleoproterozoic Vargfors syncline, Skellefte mining district, Sweden, Precambrian Res., 191, 166–183, 2011.

Bauer, T. E., Sarlus, Z., Lynch, E. P., Martinsson, O., Wanhainen, C., Drejing-Caroll, D., and Coller, D.: Two independent tectonic events controlling AIO and IOCG deposits in the Gällivare area, Sweden, Proceedings of the 14th SGA Biennal Meeting, 20–23 August, Quebec City, Canada, 839–842, 2017.

Bauer, T. E., Andersson, J. B. H., Sarlus, Z., Lund, C., and Kearney, T.: Structural controls on the setting, shape, and hydrothermal alteration of the Malmberget iron oxide-apatite deposit, Northern Sweden, Econ. Geol., 113, 377–395, 2018.

Bergman, S.: Geology of the northern Norrbotten ore province, northern Sweden, Rapporter och Meddelanden 141, Geol. Surv. of Swe., Uppsala, 428 pp., 2018.

Bergman, S., Kübler, L., and Martinsson, O.: Description of regional geological and geophysical maps of northern Norrbotten County (east of the Caledonian orogen), Geol. Surv. of Swe., Ba56, 110 pp., 2001.

Bergman, S., Billström, K., Persson, P.-O., Skiöld, T., and Evins, P.: U-Pb age evidence of repeated Paleaoproterozoic metamorphism and deformation near the Pajala shear zone in the northern Fennoscandian Shield, GFF, 128, 7–20, 2006.

Bernal, N. F., Gleeson, S. A., Smith, M. P., Barnes, J. D., and Pan, Y.: Evidence of multiple halogen sources in scapolites from iron oxide-copper-gold (IOCG) deposits and regional Na-Cl metasomatic alteration, Norrbotten County, Sweden, Chem. Geol., 451, 90–103, 2017.

Billström, K., Eilu, P., Martinsson, O., Niiranen, T., Broman, C., Weihed, P., Wanhainen, C., and Ojala, J.: IOCG and related mineral deposits of the northern Fennoscandian Shield, in: Hydrothermal iron oxide copper gold and related deposits: A global perspective, Vol. 3, edited by: Porter, T. M., PGC Publishing, Adelaide, 381–414, 2010.

Bingen, B., Solli, A., Viola, G., Torgersen, E., Svandstad, J. S., Whitehouse, M. J., Rør, J. S., Ganerød, M., and Nasuti, A.: Geochronology of the Paleoproterozoic Kautokeino Greenstone Belt: Tectonic implications in a Fennoscandia context, Norw. J. Geol., 95, 365–396, 2015.

Blatt, H., Tracy, R. J., and Owens, B. E. (Eds.): Petrology, igneous, sedimentary and metamorphic, W.H. Freeman and Company, New York, 530 pp., 2006.

Carlon, C. J.: Iron oxide systems and base metal mineralisation in northern Sweden, in: Hydrothermal iron oxide copper gold and related deposits: A global perspective, Vol. 1, edited by: Porter, T. M., PGC Publishing, Adelaide, 283–296, 2000.

Cliff, R. A., Rickard, D., and Blake, K.: Isotope systematics of the Kiruna magnetite ores, Sweden: Part 1, age of the ore, Econ. Geol., 85, 1770–1776, 1990.

Corriveau, L. and Mumin, H. (Eds.): Exploring for iron oxide copper-gold deposits: Canada and global analogues, short course notes, Vol. 20, 185 pp., Geol. Ass. of Can., St. John's, 2010.

Corriveau, L., Montreuil, J. F., and Potter, E. G.: Alteration facies linkages among iron oxide copper-gold, iron oxide-apatite, and affiliated deposits in the Great Bear Magmatic Zone, Northwest Territories, Canada, Econ. Geol., 111, 2045–2072, 2016.

Craveiro, G. S., Xavier, R. P., and Villas, R. N. N.: The Cristalino IOCG deposit: an example of multi-stage events of hydrothermal alteration and copper mineralization, Braz. J. Geol., 49, 1–18, 2019.

Debras, C.: Petrology, geochemistry, and structure for the host rock of the Printzskiöld ore body in the Malmberget deposit, MSc thesis, Luleå University of Technology, Sweden, 48 pp., 2010.

deMelo, G. H. C., Monteiro, L. V., Xavier, R. P., Moreto, C. P. N., Santiago, E. S. B., Dufrane, S. A., Aires, B., and Santos, A. F. F.: Temporal evolution of the giant Salobo IOCG deposit, Carajás Province (Brazil): constraints from paragenesis of hydrothermal alteration and U-Pb geochronology, Miner. Deposita, 52, 709–732, 2017.

Edfelt, Å.: The Tjårrojåkka apatite-iron and Cu (-Au) deposits, northern Sweden, PhD thesis, Luleå University of Technology, Sweden, 24 pp., 2007.

Edfelt, Å., Armstrong, R. N., Smith, M., and Martinsson, O.: Alteration paragenesis and mineral chemistry of the Tjårrojåkka apatite-iron and Cu (-Au) occurrences, Kiruna area, northern Sweden, Miner. Deposita, 40, 409–434, 2005.

Edfelt, Å., Sandrin, A., Evins, P., Jeffries, T., Storey, C., Elming, S.-Å., and Martinsson, O.: Stratigraphy and tectonic setting of the host rocks to the Tjårrojåkka Fe-oxide Cu-Au deposits, Kiruna area, northern Sweden, GFF, 128, 221–232, 2006.

Forsell, P.: The stratigraphy of the Precambrian rocks of the Kiruna district, northern Sweden, Geol. Surv. of Swe., C812, 36 pp., 1987.

Frietsch, R.: The Ekströmsberg iron ore deposit, northern Sweden, C708, 52 pp., Geol. Surv. of Swe., Stockholm, 1974.

Frietsch, R.: Petrochemistry of iron ore-bearing metavolcanics in Norrbotten County, northern Sweden, C802, 62 pp., Geol. Surv. of Swe., Uppsala, 1984.

Frietsch, R., Nylund, B., and Oldeberg, H.; Ekströmsberg järnmalmsfyndighet, rapport rörande resultaten av SGU:s undersökningar 1961–1969, BRAP 786, 150 pp., Geol. Surv. of Swe., Malmbyrån, 1974.

Frietsch, R., Tuisku, P., Martinsson, O., and Perdahl, J.-A.: Early Proterozoic Cu-(-Au) and iron deposits associated with regional Na-Cl metasomatism in northern Fennoscandia, Ore Geol. Rev., 12, 1–34, 1997.

Gaal, G. and Gorbatschev, R.: An outline of the Precambrian evolution of the Baltic Shield, Precambrian Res., 35, 15–52, 1987.

Geijer, P.: Igneous rocks and iron ores of Kiirunavaara, Loussavaara and Toullavaara, Scientific and practical researches in Lappland arranged by Loussavaara-Kiirunavaara Aktiebolag, 278 pp., Kungliga boktryckeriet. P. A. Norstedt & Söner, Stockholm, 1910.

Geijer, P.: Toullavaara malmfälts geologi, Geol. Surv. of Swe., C296, 49 pp., Kungliga boktryckeriet. P. A. Norstedt & Söner, Stockholm, 1920.

Geijer, P.: Gällivare Malmfält (Geology of the Gällivare ore field), Geol. Surv. of Swe., Ca22, 115 pp., Kungliga boktryckeriet. P. A. Norstedt & Söner, Stockholm, 1930.

Geijer, P.: The Rektor ore body, Geol. Surv. of Swe., C514, 18 pp., Kungliga boktryckeriet. P. A. Norstedt & Söner, Stockholm, 1950.

Grigull, S., Berggren, R., Jönnberger, J., Jönsson, C., Hellström, S., and Luth, S.: Folding observed in Paleoproterozoic supracrustal rocks in northern Sweden, in: Geology of the northern Norrbotten ore province, northern Sweden, edited by: Bergman, S., Rap-

porter och Meddelanden 141, 205–258, Geol. Surv. of Swe., Uppsala, 2018.

Hanski, E. J., Humha, H., and Melezhik, V. A.: New isotopic and geochemical data from the Paleoproterozoic Pechenga Greenstone Belt, NW Russia: Implication for basin development and duration of the volcanism, Precambrian Res., 245, 51–65, 2012.

Högdahl, K., Andersson, U. B., and Eklund, O.: The Transcandinavian Igneous Belt (TIB) in Sweden: a review of its character and evolution, Special Paper 37, 125 pp., Geol. Surv. of Fin., Espoo, 2004.

Kathol, B. and Hellström, F.: U–Pb zircon age of a quartz monzonite from Sjávnjaluokta, northern Sweden – type area for the Perthite monzonite suite, SGU Rapport 20:2018, 15 pp., Geol. Surv. of Swe., Uppsala, 2018.

Kesler, S. E.: Ore-forming fluids, Elements, 1, 13–18, 2005.

Kolb, J., Vennemann, T., Meyer, F. M., and Hoffbauer, R.: Geological setting of the Guelb Moghrein Fe Oxide-Cu-Au-Co mineralization, Akjoujt area, Mauritania, in: The boundaries of the West African Craton, edited by: Ennih, N. and Liégeois, J.-P., Special publications, 297, 53–75, Geological Society, London, 2008.

Kumpulainen, R.: Guide for geological nomenclature in Sweden, GFF, 139, 3–20, 2007.

Lahtinen, R., Korja, R., and Nironen, M.: Paleoproterozoic tectonic evolution, in: Precambrian Geology of Finland – key to the evolution of the Fennoscandian Shield, Vol. 14, edited by: Lehtinen, M., Nurmi, P. A., and Rämö, O. T., Elsevier, Amsterdam, 481–532, 2005.

Lahtinen, R., Garde, A. A., and Melezhik, V. A.: Paleoproterozoic evolution of Fennoscandia and Greenland, Episodes, 31, 1–9, 2008.

LKAB: LKAB Annual Report, available at: https://www.lkab.com/en/SysSiteAssets/documents/finansiell-information/en/annual-reports/lkab_2017_annual_and_sustainability_report.pdf (last access: 7 April 2020), 2017.

Luth, S., Jönnberger, J., and Grigull, S.: The Vakko and Kovo Greenstone belts: Integrating structural geological mapping and geophysical modelling, in: Geology of the northern Norrbotten ore province, northern Sweden, edited by: Bergman, S., Rapporter och Meddelanden 141, 287–310, Geol. Surv. of Swe., Uppsala, 2018.

Lynch, E. P., Jönnberger, J., Bauer, T. E., Sarlus, Z., and Martinsson, O.: Meta-volcanosedimentary rocks in the Nautanen area, Norrbotten: preliminary lithological and deformation characteristics, SGU-rapport 30:2015, 51 pp., Geol. Surv. of Swe., Uppsala, 2015.

Lynch, E. P., Hellström, F. A., Huhma, H., Jönnberger, J., Persson, P.-O., and Morris, G. A.: Geology, lithostratigraphy and petrogenesis of c. 2.14 Ga greenstones in the Nunasvaara and Masugnsbyn areas, northernmost Sweden, in: Geology of the northern Norrbotten ore province, northern Sweden, edited by: Bergman, S., Rapporter och Meddelanden 141, 19–78, Geol. Surv. of Swe., Uppsala, 2018a.

Lynch, E. P., Bauer, T. E., Jönnberger, J., Sarlus, Z., Morris, G. A., and Persson, P.-O.: Petrological and structural character of c. 1.88 Ga meta-volcanosedimentary rocks hosting iron oxide-copper-gold and related mineralisation in the Nautanen-Aitik area, northern Sweden, in: Geology of the northern Norrbotten ore province, northern Sweden, edited by: Bergman, S., Rapporter och Meddelanden 141, 107–150, Geol. Surv. of Swe., Uppsala, 2018b.

Martinsson, O.: Tectonic setting and metallogeny of the Kiruna greenstones, PhD thesis, Luleå University of Technology, Sweden, 165 pp., 1997.

Martinsson, O.: Geology and metallogeny of the northern Norrbotten Fe-Cu-Au province, in: Svecofennian ore-forming environments of northern Sweden – volcanic associated Zn-Cu-Au-Ag, intrusion related Cu-Au, sediment hosted Pb-Zn, and magnetite-apatite deposits in northern Sweden, edited by: Allen, R. L., Martinsson, O., and Weihed P., Guide book series, 33, 131–148, Soc. of Econ. Geol., Littleton, USA, 2004.

Martinsson, O., Billström, K., Broman, C., Weihed, P., and Wanhainen, C.: Metallogeny of the Northern Norrbotten Ore Province, Northern Fennoscandian Shield with emphasis on IOCG and apatite-iron ore deposits, Ore Geol. Rev., 78, 447–492, 2016.

Melezhik, V. A. and Fallick, A.: On the Lomagundi-Jatuli carbon isotopic event: The evidence from the Kalix Greenstone Belt, Sweden, Precambrian Res., 179, 165–190, 2010.

Melezhik, V. A. and Hanski, E.: The early Proterozoic of Fennoscandia: Geological and tectonic settings, in: Reading the archives of earth oxygenation, Vol. 1, edited by: Melezhik, V., Prave, A. R., Hanski, E. J., Fallick, A. E., Lepland, A., Kump, L. R., Strauss, H., Springer, Berling, 33–38, 2012.

Montreuil, J.-F., Corriveau, L., Potter, E. G., and De Toni, A. F.: On the relationship between alteration facies and metal endowment of iron oxide-alkali-altered systems, Southern Great Bear Magmatic Zone (Canada), Econ. Geol., 111, 2139–2168, 2016.

New Boliden AB: New Boliden AB Annual Report, available at: https://vp217.alertir.com/afw/files/press/boliden/201803060710-1.pdf (last access: 7 April 2020), 2017.

OECD: OECD Territorial Reviews: Northern Sparsely Populated Areas, OECD publishing, Paris, 190 pp., 2017.

Offerberg, J.: Beskrivning till berggrundskartbladen Kiruna NV, NO, SV, SO, Af 1–4, 147 pp., Geol. Surv. of Swe., Stockholm, 1967.

Öhlander, B., Hamilton, P. J., Fallick, A. E., and Wilson, M. R.: Crustal reactivation in northern Sweden: the Vettasjärvi Granite, Precambrian Res., 35, 277–293, 1987.

Parák, T.: The origin of the Kiruna iron ores, C709, 209 pp., Geol. Surv. of Swe., Stockholm, 1975.

Passchier, C. W. and Trouw, R. A. J. (Eds.): Microtectonics, Springer-Verlag, Berlin Heidelberg, 366 pp., 2005.

Perdahl, J.-A. and Frietsch, R.: Petrochemical and petrological characteristics of 1.9 Ga old metavolcanics in northern Sweden, Precambrian Res., 64, 239–252, 1993.

Pharaoh, T. C. and Pearce, J. A.: Geochemical evidence for the geotectonic setting of early Proterozoic metavolcanic sequences in Lapland, Precambrian Res., 25, 283–308, 1984.

Romer, R.: U-Pb systematics of stilbite-bearing low-temperature mineral associations from the Malmberget iron ore, northern Sweden, Geochim. Cosmochim. Ac., 60, 1951–1961, 1996.

Romer, R., Martinsson, O., and Perdahl, J.-A.: Geochronology of the Kiruna iron ores and related hydrothermal alteration, Econ. Geol., 89, 1249–1261, 1994.

Ros, F.: Tjårrojåkka kopparmalmsfyndighet, Geol. Surv. of Swe., BRAP 82567, 13 pp., 1979.

Rutanen, H. and Andersson, U. B.: Mafic plutonic rocks in a continental-arc setting: Geochemistry of 1.87–1.78 Ga rocks from south-central Sweden and models of their palaeotectonic setting, Geol. J., 44, 241–279, 2009.

Sandrin, A. and Elming, S.-Å.: Geophysical and petrophysical study of an iron oxide copper gold deposit in northern Sweden, Ore Geol. Rev., 29, 1–18, 2006.

Sarlus, Z., Andersson, U. B., Bauer, T. E., Wanhainen, C., Martinsson, O., Nordin, R., and Andersson, J. B. H.: Timing of plutonism in the Gällivare area: Implications for Proterozoic crustal development in the northern Norrbotten mining district, Sweden, Geol. Mag., 155, 1–26, 2017.

Sarlus, Z., Martinsson, O., Bauer, T. E., Wanhainen, C., Andersson, J. B. H., and Nordin, R.: Character and tectonic setting of plutonic rocks in the Gällivare area, northern Norrbotten, Sweden, GFF, 141, 1–20, 2019.

Skelton, A., Mansfeld, J., Ahlin, S., Lundqvist, T., Linde, J., and Nilsson, J.: A compilation of metamorphic pressure-temperature estimates from the Svecofennian province of eastern and central Sweden, GFF, 140, 1–10, 2018.

Skiöld, T.: U-Pb zircon and Rb-Sr whole-rock and mineral ages of Proterozoic intrusives on map sheet Lannavaara, north-eastern Sweden, GFF, 101, 131–137, 1979.

Skirrow, R. G., Murr, J., Schofield, A., Huston, D. L., van der Wielen, S., Czarnota, K., Coghlan, R., Highet, L. M., Connolly, D., Doublier, M., and Duan, J.: Mapping iron oxide Cu-Au (IOCG) mineral potential in Australia using a knowledge-driven mineral systems-based approach, Ore Geol. Rev., 113, 103011, https://doi.org/10.1016/j.oregeorev.2019.103011, 2019.

Skyttä, P., Bauer, T. E., Tavakoli, S., Hermansson, T., Andersson, J., and Weihed, P.: Pre-1.87 Ga development of crustal domains overprinted by 1.87 Ga transpression in the Paleoproterozoic Skellefte-district, Sweden, Precambrian Res., 206–207, 109–136, 2012.

Smith, M., Coppard, J., Herrington, R., and Stein, H.: The geology of the Rakkurijärvi Cu-(Au)-prospect, Norrbotten: A new iron oxide copper gold deposit in northern Sweden, Econ. Geol., 102, 393–414, 2007.

Smith, M. P., Storey, C. D., Jeffries, T. E., and Ryan, C.: In situ U-Pb and trace element analysis of accessory minerals in the Kiruna district, Norrbotten, Sweden: New constraints on timing and origin of mineralization, J. Petrol., 50, 2063–2094, 2009.

Spear, F. S. (Ed.): Metamorphic phase equilibria and pressure-temperature-time path, Miner. Ass. of Amer., Washington, 799 pp., 1993.

Talbot, C. J. and Koyi, H.: Paleoproterozoic intraplating exposed by resultant gravity overturn near Kiruna, northern Sweden, Precambrian Res., 72, 199–225, 1995.

Tollefsen, E.: Thermal and chemical variations in metamorphic rocks in Nautanen, Gällivare, Sweden, MSc thesis, Stockholm University, Sweden, 50 pp., 2014.

Vollmer, F. W., Wright, S. F., and Hudleston, J. P.: Early deformation in the Svecokarelian greenstone belt in the Kiruna iron district, northern Sweden, GFF, 106, 109–118, 1984.

Wanhainen, C., Billström, K., Martinsson, O., Stein, H., and Nordin, R.: 160 Ma of magmatic/hydrothermal and metamorphic activity in the Gällivare area: Re–Os dating of molybdenite and U–Pb dating of titanite from the Aitik Cu–Au–Ag deposit, northern Sweden, Miner. Deposita, 40, 435–447, 2005.

Wanhainen, C., Broman, C., Martinsson, O., and Magnor, B.: Modification of a Paleoproterozoic porphyry-like system: Integration of structural, geochemical, petrographic, and fluid inclusion data from the Aitik Cu–Au–Ag deposit, northern Sweden, Ore Geol. Rev., 48, 306–331, 2012.

Weihed, P., Billström, K., Persson, P.-O., and Bergman-Weihed, J.: Relationship between 1.90-1.85 Ga accretionary processes and 1.82–1.80 Ga oblique subduction at the Karelian craton margin, Fennoscandian Shield, GFF, 124, 163–180, 2002.

Weihed, P., Eilu, P., Larsen, R. B., Stendal, H., and Tontti, M.: Metallic mineral deposits in the Nordic countries, Episodes, 31, 125–132, 2008.

Welin, E., Christiansson, K., and Nilsson, Ö.: Rb-Sr radiometric ages of extrusive and intrusive rocks in northern Sweden, C666, 38 pp., Geol. Surv. of Swe., Stockholm, 1971.

Westhues, A., Hanchar, J. M., Whitehouse, M. J., and Martinsson, O.: New constraints on the timing of host rock emplacement, hydrothermal alteration and iron oxide-apatite mineralization in the Kiruna district, Norrbotten, Sweden, Econ. Geol., 111, 1595–1618, 2016.

Westhues, A., Hanchar, J. M., Voicey, C. R., Whitehouse, M. J., Rossman, G. R., and Wirth, R.: Tracing the fluid evolution of the Kiruna iron oxide deposits using zircon, monazite, and whole rock trace elements and isotopic studies, Chem. Geol., 466, 303–322, 2017.

Witschard, F.: Description of the geological maps Fjällåsen NV, NO, SV, SO, Af 17-20, 125 pp., Geol. Surv. of Swe., Stockholm, 1975.

Wright, S. F.: Early Proterozoic deformational history of the Kiruna district, northern Sweden, PhD thesis, University of Minnesota, USA, 170 pp., 1988.